alloys

MDPI

Review

Applications, Mechanisms, and Key Technical Challenges of Rare Earth Elements in Weathering Steels

Jun Cai [1], Libin Yang [2,*], Liping Wu [3], Jie Wang [2], Wei Wu [2] and Bo Zhao [2]

[1] State Key Laboratory of Advanced Metallurgy, University of Science and Technology Beijing, Beijing 100083, China; m17801186227@163.com
[2] Metallurgical Technology Department, Central Iron and Steel Research Institute Co., Ltd., Beijing 100081, China; xianglei521588@163.com (J.W.); wuweineu@163.com (W.W.); zhaobo_working@163.com (B.Z.)
[3] Materials Science and Engineering, Inner Mongolia University of Technology, Hohhot 010051, China; 2023910612@imut.edu.cn
* Correspondence: libyangz@126.com

Abstract

Weathering steels have been widely used in transportation, energy facilities, and civil infrastructure because of their good atmospheric corrosion resistance and long service life. Their corrosion resistance is generally achieved by adding alloying elements such as Cu, P, Cr, and Ni, which promote the formation of a stable and protective rust layer. Among these elements, however, Ni and Cr are relatively expensive and their resources are limited. Therefore, reducing the use of Ni and Cr while maintaining good corrosion resistance has become an important issue in the development of weathering steels. Recent studies have demonstrated that rare-earth elements can markedly improve the corrosion resistance of steels through multiple mechanisms, including optimization of rust-layer structure, microstructural refinement, inclusion modification, and regulation of grain-boundary characteristics. Rare-earth microalloying therefore provides an effective approach to reducing the consumption of conventional alloying elements in weathering steels. This paper systematically reviews the corrosion mechanisms of weathering steels, the evolution of rust-layer structures, and the roles of alloying elements, with particular emphasis on the effects of Cu, P, Cr, and Ni on the densification and stabilization of rust layers. The microalloying effects of rare-earth elements, their inclusion-modification behavior, and their deoxidation and desulfurization mechanisms are also summarized, and their roles in reducing pitting susceptibility and promoting the formation of stable protective rust layers are clarified. In addition, the occurrence states of rare-earth elements in steel and their effects on performance stability are discussed. Key challenges encountered in the industrial application of rare-earth steels, including fluctuations in rare-earth yield and continuous-casting nozzle clogging, are also summarized. The available evidence indicates that the effective application of rare-earth elements in weathering steels remains constrained by molten-steel cleanliness, inclusion control, and the stability of continuous-casting operations. Future research should focus on technologies for the stable addition and controlled occurrence of rare-earth elements under low-oxygen and low-sulfur smelting conditions, thereby enabling the efficient utilization and stable industrial application of abundant rare-earth resources in weathering steels.

Keywords: weathering steel; rare-earth microalloying; rust-layer structure; inclusion modification; pitting corrosion behavior; continuous-casting castability

Check for updates

Academic Editor: Hardy Mohrbacher

Received: 13 July 2026
Revised: 7 August 2026
Accepted: 24 August 2026
Published: 1 September 2026

Copyright: © 2026 by the authors. Licensee MDPI, Basel, Switzerland. This article is an open access article distributed under the terms and conditions of the Creative Commons Attribution (CC BY) license.

1. Introduction

Weathering steel has been widely used in transportation, energy and marine engineering, bridges, buildings, engineering machinery and other outdoor structures due to its good corrosion resistance and long service life. In the atmospheric environment, especially under the conditions of humidity, salt fog, industrial pollution and repeated wet and dry cycles, ordinary carbon steel may suffer serious corrosion. Continuous corrosion will cause material loss and cross-section thinning, which will gradually reduce the bearing capacity and reliability of steel structures, and increase maintenance and replacement requirements. The weathering steel has both corrosion resistance and mechanical properties and welding properties required for structural applications, which provides a feasible solution to solve the above problems. Therefore, in the whole life cycle of the structure, the application of weathering steel can reduce maintenance requirements and steel consumption.

The corrosion resistance of weathering steel is closely related to its alloy composition. Cu, P, Cr, Ni and Ti are usually added to promote the formation of a dense and stable rust layer and improve the microstructure of the steel. In recent years, rare earth (RE) elements have attracted more and more attention because of their role in improving the cleanliness of molten steel, regulating inclusions, improving microstructure and corrosion behavior. These alloying methods provide effective means to improve the service performance of weathering steel in atmospheric corrosion environment from different ways. Among these elements, Cr and Ni can promote the formation of a dense protective rust layer and are therefore important alloying elements for improving corrosion resistance. However, Ni and Cr resources are relatively scarce in China, and their alloying costs are relatively high. Excessive additions also increase steel production costs. Therefore, in the development of high-performance weathering steels, maintaining or even further improving corrosion resistance while reducing the use of expensive alloying elements such as Ni and Cr is a key issue that needs to be addressed in the compositional design and industrial production of weathering steels.

With the increasing application of rare-earth elements in steel materials, it is generally recognized that rare-earth elements can significantly improve the corrosion resistance of ordinary carbon steels and low-alloy steels. Rare-earth elements are chemically active and possess strong deoxidation, desulfurization, and inclusion-modification capabilities. After being added to steel, rare-earth elements can improve the toughness, corrosion resistance, fatigue performance, and heat resistance of steel through multiple effects, including improving the solidification structure, refining the microstructure formed during solid-state phase transformation, modifying and refining inclusions, strengthening grain boundaries and phase boundaries through segregation, and promoting the densification and stabilization of the rust layer. Among them, cerium and lanthanum are light rare-earth elements with relatively high abundances in the Earth's crust. They have high resource availability and relatively low costs, providing a sound basis for their application and broader use in the metallurgical industry.

Although the mechanisms and application effects of rare-earth elements in steel have been widely reported, most existing conclusions are derived from laboratory studies or small-scale trials, and research on the industrial production of weathering steels with relatively high rare-earth contents remains insufficient. Rare earth elements have a strong affinity for oxygen and sulfur in molten steel, and are easy to form rare earth oxides, sulfides and oxygen sulfides. Therefore, in the process of steelmaking, the yield of rare earth elements often fluctuates greatly, and its solid solubility is also difficult to achieve stable control. These fluctuations may weaken the expected effect of adding rare earth on improving the corrosion resistance of weathering steel. Meanwhile, during continuous casting, rare-earth inclusions tend to deposit on the inner wall of the nozzle, causing nozzle

clogging or restricted flow and affecting the number of heats in a casting sequence and production efficiency. Therefore, the stable addition of rare-earth elements to steel, control of their occurrence states, improvement of their yield, and enhancement of continuous-casting castability are key issues restricting the stable and large-scale production of rare-earth weathering steels.

In response to the practical demands for the comprehensive utilization of high-abundance rare-earth resources from the Bayan Obo deposit and for the development of high-performance, low-cost weathering steels, the advantages of steel materials—including their large consumption, wide range of applications, and strong capacity for the large-scale utilization of rare-earth resources—should be fully exploited. Combining the corrosion-resistance-enhancing effects of rare-earth elements with the development of weathering-steel products and conducting research on stable rare-earth addition to molten steel, rare-earth yield control, regulation of rare-earth occurrence states, and improvement of continuous-casting castability will help overcome the bottlenecks in the industrial production of rare-earth weathering steels and enable the high-value and large-scale application of high-abundance rare-earth resources in steel materials.

2. Factors Affecting the Performance of Weathering Steel

2.1. Corrosion-Resistance Mechanism of Weathering Steel

Weathering steel, also known as atmospheric corrosion-resistant steel, is a type of low-alloy high-strength steel that exhibits excellent resistance to atmospheric corrosion through the addition of small amounts of alloying elements. Its development history is illustrated in Figure 1. As early as 1900, scientists in Europe and the United States found that Cu could significantly improve the atmospheric corrosion resistance of steel. In 1933, the United States Steel Corporation successfully developed the Cor-Ten series of weathering steels for the first time, which were mainly used in the manufacture of railway vehicles [1]. Compared with ordinary carbon steel, Cor-Ten steel exhibited a 30% improvement in mechanical properties, together with a significant enhancement in corrosion resistance.

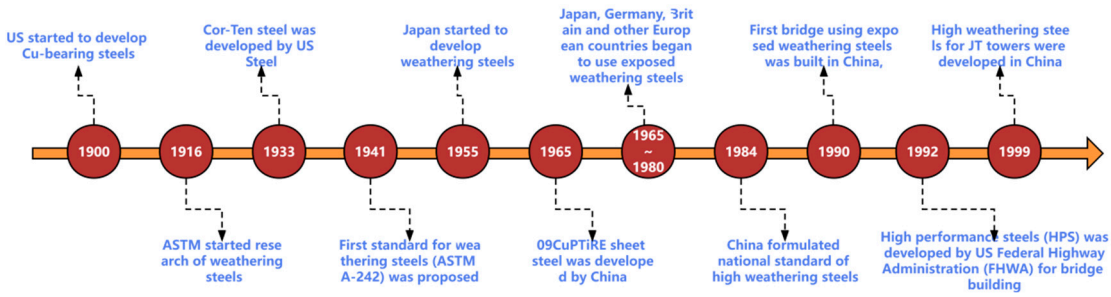


Figure 1. Development history of weathering steel in the 20th century.

In 1941, the United States established the first weathering steel standard, ASTM A-242. In 1965, China successfully developed 09CuPTiRE weathering steel. In 1968, according to differences in P content, weathering steel was further classified into two categories: Cor-Ten A, with a P mass fraction of 0.07–0.15%, and Cor-Ten B, with a P mass fraction of no more than 0.04% [2,3]. China established its national standard for weathering steel in 1984.

In 1992, the Federal Highway Administration (FHWA), the American Iron and Steel Institute (AISI), and the United States Navy jointly developed high-performance steel (HPS) for bridge construction. HPS improves weldability by reducing the contents of C, P, and S, while increasing the upper limit of Mn content to improve fracture toughness and yield strength. It also forms a protective rust layer, thereby enhancing corrosion resistance [4]. Nippon Steel Corporation introduced the Cor-Ten series of weathering steels

and subsequently developed various weathering steels suitable for different applications. Since then, weathering steel has been widely used in construction facilities, bridges, vehicle manufacturing, and other fields in Europe, the United States, Japan, and other countries [5].

In atmospheric environments, steel corrosion is jointly caused by various chemical, electrochemical, and physical processes occurring at the interfaces among the gas, liquid, and solid phases, among which electrochemical corrosion plays the dominant role. Regarding the corrosion-resistance mechanism of weathering steel, when the steel surface comes into contact with the atmosphere, H^+ or O_2 in the liquid film undergoes reduction at the cathode, thereby driving the electrochemical reactions. The atmospheric corrosion resistance of weathering steel is mainly developed through the following three stages [6]:

(1) Formation of an ordinary rust layer

When weathering steel is exposed to the atmosphere, a thin film forms on the steel surface. This film contains gases such as CO_2, SO_2, NO_x, H_2S, and NH_3, as well as salt ions such as Cl^- and HSO_3^-. These substances cause the film to act as an electrolyte solution, resulting in anodic dissolution. Initially, a γ-FeOOH rust layer similar to that formed on ordinary carbon steel is generated.

(2) Stable propagation of corrosion

After 3–5 years of environmental corrosion, the rust layer adjacent to the steel substrate continuously dissolves and reprecipitates, forming a relatively dense amorphous oxyhydroxide [5].

(3) Formation of a stable rust layer

After many years, atmospheric corrosion-resistant steel eventually develops a stable rust layer. The inner rust layer, which provides the main protective effect, consists of α-FeOOH enriched with elements such as Cr, Cu, N, and P, as shown in Figure 2.

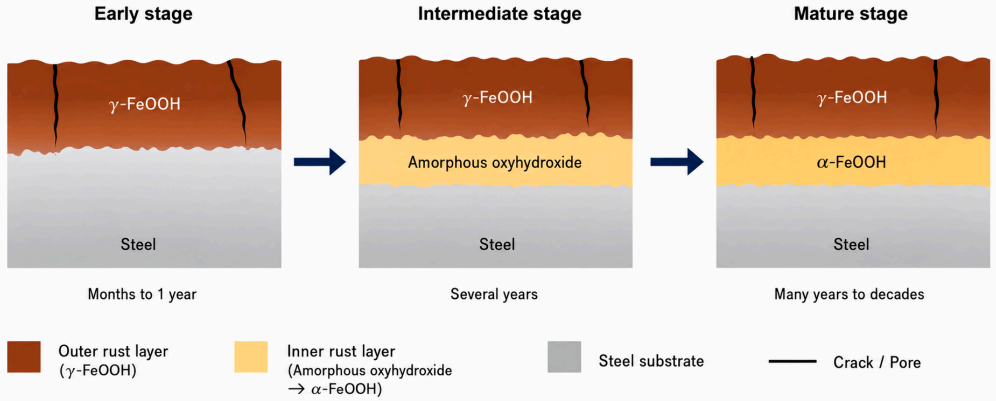


Figure 2. Schematic diagram of rust-layer transformation in weathering steel. Adapted from Ref. [6].

2.2. Effect of Rust-Layer Composition on the Properties of Weathering Steel

The composition, properties, and structure of the rust layer have a significant influence on the corrosion resistance of steel, and the phase composition of the rust layer is highly complex. After stabilization, the rust layer formed on the surface of weathering steel can be divided into inner and outer layers. The outer layer is loose and porous and mainly consists of γ-FeOOH, whereas the inner layer is dense and mainly consists of α-FeOOH. The corrosion resistance of the rust layer is primarily attributed to the inner layer, and alloying elements also improve the corrosion resistance of weathering steel through their effects on the inner rust layer.

Researchers have investigated the rust-layer compositions of different weathering steels. Han [7] compared the corrosion behaviors of weathering steel and Q235 steel in industrial and rural environments, as shown in Figure 3. It was found that the corrosion products of weathering steel contained higher amounts of α-FeOOH, CuO, and Ni com-

pounds, making its rust layer denser than that of Q235 steel and thereby providing higher corrosion resistance. Du [8] investigated the atmospheric corrosion behaviors of 921A steel and Q450NQR1 steel and found that 921A steel exhibited better corrosion resistance than Q450NQR1 steel under simulated severe atmospheric conditions. The corrosion products of both steels consisted of α-FeOOH, Fe_3O_4, and γ-FeOOH, among which α-FeOOH was more abundant in the rust layer of 921A steel than in that of Q450NQR1 steel. The inner rust layer of 921A steel also exhibited co-enriched regions of Cr, Ni, Mo, and V, resulting in superior corrosion resistance compared with Q450NQR1 steel.

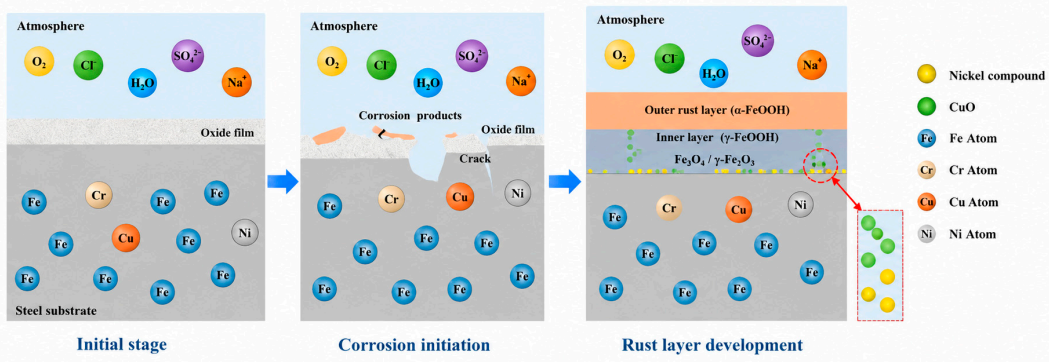


Figure 3. Schematic diagram of the corrosion process of weathering steel.

In summary, with respect to iron oxides, loose γ-FeOOH is formed during the initial stage of corrosion, whereas dense α-FeOOH forms at the later stage. The formation of a dense α-FeOOH rust layer is the main reason for the corrosion resistance of steel.

Previous studies have also investigated the effects of different elements on the weathering resistance of steel. Fan [9] investigated the effect of Cu addition on the microstructural evolution and material transformation of the corrosion product layer through comprehensive microscopic characterization and immersion tests, as shown in Figure 4. The oxides formed by the added Cu provided nucleation sites for the formation of $CuFeO_2$, and $CuFeO_2$ enhanced the ability of the corrosion product layer to block Cl^- penetration. Wang et al. [10] reported that rare-earth addition improved the corrosion resistance of carbon steel by promoting the formation of compact rust layers with increased α-FeOOH content and reduced unstable iron oxyhydroxide phases. Yamashita et al. [11] found that, after long-term exposure for 0.5–26 years, the surface of weathering steel became dark brown, and the inner rust layer was dense and mainly composed of compact α-FeOOH nanoparticles adsorbed on the steel surface. The inner rust layer contained a considerable amount of Cr, while no Si penetration was observed, thereby protecting the weathering steel substrate from attack by atmospheric corrosive media. Zhang [12] found that, after one year of exposure, the outer rust layer of weathering steel was mainly composed of FeO, $Fe(OH)_2$, and γ-FeOOH, whereas the inner rust layer was mainly composed of α-FeOOH. Cr enrichment was observed at cracks in the inner rust layer, which could improve the performance of weathering steel.

In summary, regarding the effects of alloying elements on weathering resistance, alloying elements such as Cu, Ni, rare earths, and P can promote the formation of α-FeOOH, thereby increasing the compactness of the inner rust layer. Meanwhile, these alloying elements can become enriched in the inner rust layer, where they form certain spinel-type compounds, substitute for Fe atoms at specific lattice sites, or form interstitial solid solutions. These effects improve the properties and structure of the rust layer and consequently enhance the corrosion resistance of weathering steel.

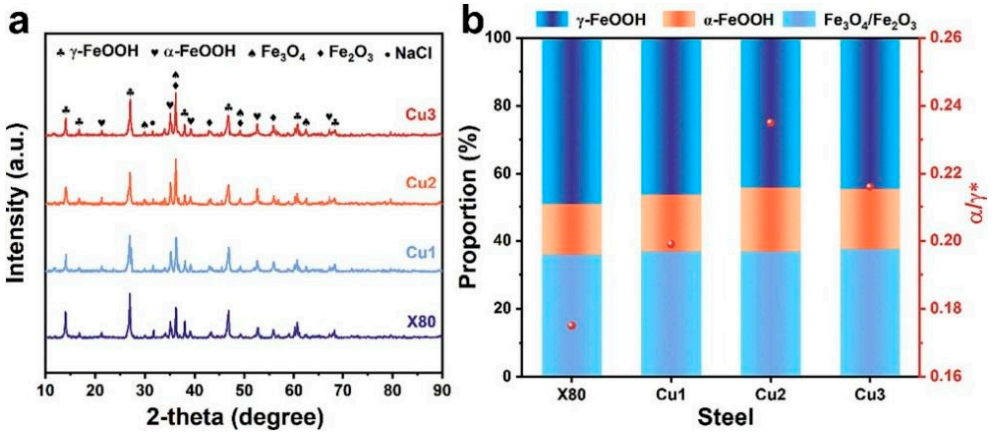


Figure 4. Phase composition of the rust layers of Cu-containing and Cu-free steels. (**a**) XRD analysis of corrosion products; (**b**) ratios of γ-FeOOH, α-FeOOH, and Fe_3O_4/Fe_2O_3, as well as the α/γ* ratio.

2.3. Effect of Inclusion Types on the Properties of Weathering Steel

Common inclusions in steel include MnS, Al_2O_3, CaS, TiN, Ca–Al–Mg–O, and Ca–Al–Mg–Si–O inclusions. The influence of inclusions on steel properties mainly depends on whether they readily induce pitting corrosion. Extensive studies have been conducted on the effects of inclusion types on the properties of weathering steels and stainless steels. The effects of different inclusions on weathering resistance are summarized in Table 1.

Table 1. Mechanisms by which various inclusions in steel affect corrosion resistance.

Reference	Steel Grade	Inclusion Type	Effect on the Properties of Weathering Steel
[13]	Stainless steel	MnS and CaS inclusions	Effective pitting initiators that can act as preferential initiation sites.
[14]	Super duplex stainless steel	MnS inclusions	Partial dissolution of MnS produces an acidic corrosive environment, resulting in partial dissolution of the amorphous oxide phase.
[15]	P110 oil casing steel	CaS–$MgAl_2O_4$ inclusions and ZrO_2-containing inclusions	Stable ZrO_2 inclusions effectively inhibit inclusion-induced localized corrosion.
[16]	321 stainless steel	TiN inclusions	Pure TiN has no effect on pitting corrosion, whereas CaS within TiN inclusions is the actual initiator of pitting corrosion.
[17]	Stainless steel	MnS and Al–Mg–Ca–O inclusions	Dissolution of the inclusions causes pitting corrosion.
[18]	DP, TWIP, and TRIP steels	MnS inclusions	MnS and Mn–O–S inclusions act as galvanic anodes in complex inclusions.
[19]	Stainless steel	CaO	MnS, CaS, and CaO inclusions are particularly detrimental to pitting corrosion resistance.
[20]	Q450NQR1 weathering steel	CaS inclusions and rare-earth oxides and sulfides in RE-modified steel	These inclusions preferentially dissolve in acidic media, thereby reducing the corrosion rate of the steel matrix.

In summary, the effects of inclusions on corrosion resistance are mainly reflected in pitting corrosion. Inclusions with a high electrochemical potential, such as MnS, CaS, CaO, Al_2O_3, and $MgAl_2O_4$ inclusions, preferentially corrode relative to the steel matrix,

thereby leading to the formation of corrosion pits. After rare-earth (RE) or Zr treatment, the electrochemical potential of the inclusions decreases, thus retarding the formation of corrosion pits.

2.4. Effect of the Occurrence Forms of Corrosion-Resistant Elements on the Properties of Weathering Steel

Weathering steel exhibits good corrosion resistance, in which alloying elements play a decisive role. In summary, alloying elements improve corrosion resistance mainly through three aspects [21–25]: reducing the electrical conductivity of the rust layer and affecting the phase structure and phase types within the rust layer; accelerating the uniform dissolution of steel, promoting the transformation of Fe^{2+} into Fe^{3+}, and delaying rust crystallization; and blocking cracks and reducing related defects.

Cu is one of the most effective alloying elements in atmospheric corrosion-resistant steel. There are mainly two viewpoints regarding the mechanism by which Cu improves the atmospheric corrosion resistance of steel [24–26]. One view is that Cu promotes anodic passivation of steel and reduces the corrosion rate. The other view is that Cu becomes enriched at the interface between the steel matrix and the rust layer, forming a protective layer mainly composed of Cu and P that is tightly bonded to the matrix. As an anodic depolarizer, P acts synergistically with Cu to accelerate the uniform dissolution of steel and promote the transformation of Fe^{2+} into Fe^{3+}, thereby facilitating the formation of a uniform rust layer. Cr can form a dense oxide film on the steel surface and improve the passivation ability of steel. Studies [1,27–29] have suggested that increasing the Cr content facilitates the refinement of α-FeOOH and effectively inhibits the penetration of corrosive Cl^-. Ni shifts the self-corrosion potential of steel in the positive direction, thereby increasing its stability. The addition of Ti and V mainly inhibits grain growth through the formation of TiN or V carbonitrides, thereby enhancing precipitation strengthening and grain-refinement strengthening in atmospheric corrosion-resistant steel. Rare-earth elements are extremely reactive. Their addition to steel is beneficial for purifying molten steel, refining dendrites, modifying the properties, morphology, and distribution of inclusions, and reducing corrosion initiation sites, thereby improving the properties of steel. Rare-earth elements can also effectively increase the nonequilibrium solute partition coefficients of elements such as P, S, and Cu [30]. The effects of different corrosion-resistant elements on weathering resistance are summarized in Table 2.

Table 2. Effects of common elements in steel on the properties of weathering steel.

References	Alloying Element	Effect	Mechanism	Characteristics
[1,21,24–26]	Cu	The addition of 0.12–0.14% Cu to steel provides strong corrosion resistance.	① Promotion of anodic passivation ② Cu enrichment mechanism	Cu has a pronounced effect in counteracting the harmful influence of S in steel.
[21]	P	One of the most effective alloying elements for improving the atmospheric corrosion resistance of steel.	P facilitates the formation of a uniform FeOOH rust layer on the steel surface and promotes the formation of a protective film.	The combined addition of P and Cu to steel produces a stronger synergistic effect.
[28–30]	Cr	Forms a dense oxide film on the steel surface and improves the passivation ability of steel.	Promotes the refinement of α-FeOOH, inhibits the penetration of Cl^- ions, and suppresses the transformation of Fe^{3+} into Fe^{2+}.	The effect is particularly pronounced when Cr and Cu are added simultaneously.
[31,32]	Ni	Shifts the self-corrosion potential of steel in the positive direction.	Ni enrichment in the rust layer effectively inhibits the penetration of Cl^- ions.	Approximately 4% Ni can significantly improve the atmospheric corrosion resistance of steel.

3. Research on the Role of Rare-Earth Elements in Weathering Steel

3.1. Effect of Rare-Earth Microalloying on Corrosion Resistance

When rare-earth elements are added to steel as microalloying elements, they may exist in the Fe lattice in the form of substitutional or interstitial solid solutions. Meanwhile, solute redistribution during solidification causes rare-earth elements to segregate at grain boundaries, and this portion of rare-earth elements may affect the corrosion resistance of steel.

Rare-earth elements in solid solution have a significant influence on corrosion resistance. On the one hand, rare-earth elements segregate at grain boundaries and form a rare-earth-enriched region between the rust layer and the steel matrix, thereby preventing corrosive ions from contacting the steel matrix. Taking microalloyed steel as an example, Zhang [33] found that the addition of RE reduced the electrochemical activity of the surface, thereby decreasing the tendency of chloride ions to adsorb on the metal surface. Zhu [34] determined through electrochemical tests that the corrosion inhibition efficiency of CeN for X70 steel could reach 98.21%. Lian [35] suggested that rare-earth atoms tend to segregate toward grain boundaries and form a rare-earth-enriched region between the rust layer and the matrix, thereby preventing corrosive ions from contacting the steel matrix.

On the other hand, rare-earth elements dissolved in the Fe lattice can promote the formation of α-FeOOH and reduce the formation of γ-FeOOH during corrosion, thereby increasing the charge-transfer resistance and improving the compactness of the rust layer. Dong [36] found that the addition of a trace amount of lanthanum, below 0.0020 wt%, increased the compactness of the corrosion product layer on offshore-platform steel, mainly by promoting the formation of α-FeOOH. Jia [37] investigated the effect of RE on the atmospheric corrosion behavior of weathering angle steel using cyclic immersion wet/dry corrosion tests. The results showed that the anodic process was inhibited during corrosion, and the resistance increased with increasing immersion time. Niu [38] found that La refined the grains, minimized the local potential differences on the matrix surface, and inhibited the oxidation of Fe_3O_4 back to γ-FeOOH during localized corrosion, thereby reducing the formation of γ-FeOOH and increasing the charge-transfer resistance. Xu [39] investigated the effect of rare-earth alloying on the corrosion of N80 steel and found that a goethite phase formed on N80RE steel, improving the compactness of the rust layer, as shown in Figure 5.

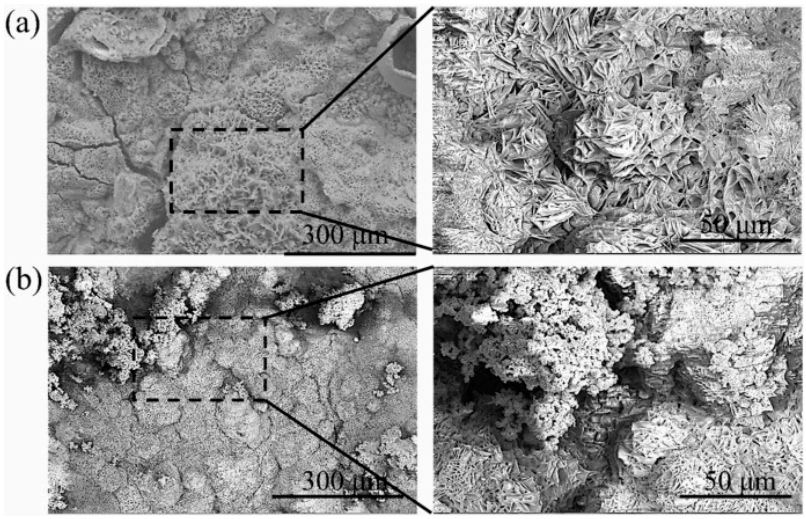


Figure 5. Microstructure of the acicular mineral phase. (**a**) SEM image of the rust layer on N80; (**b**) SEM image of the rust layer on N80RE.

3.2. Effect of Rare-Earth-Induced Inclusion Modification on Corrosion Resistance

Weathering steel must possess not only good strength and toughness but also excellent corrosion resistance. Inclusions in weathering steel may adversely affect its properties. However, the introduction of rare-earth elements can alter the characteristics and distribution of inclusions, thereby exerting a beneficial effect on corrosion resistance.

Li [40] used an independently developed three-dimensional characterization technique based on inclusion extraction to analyze the morphologies of inclusions in rare-earth-treated GCr15 bearing steel and an imported bearing steel, as shown in Figure 6. It was found that, after rare-earth addition, elongated MnS and Al_2O_3 inclusions were transformed into spherical or nearly spherical RE_2O_3 or RE_2O_2S inclusions, thereby improving the overall properties of the steel.

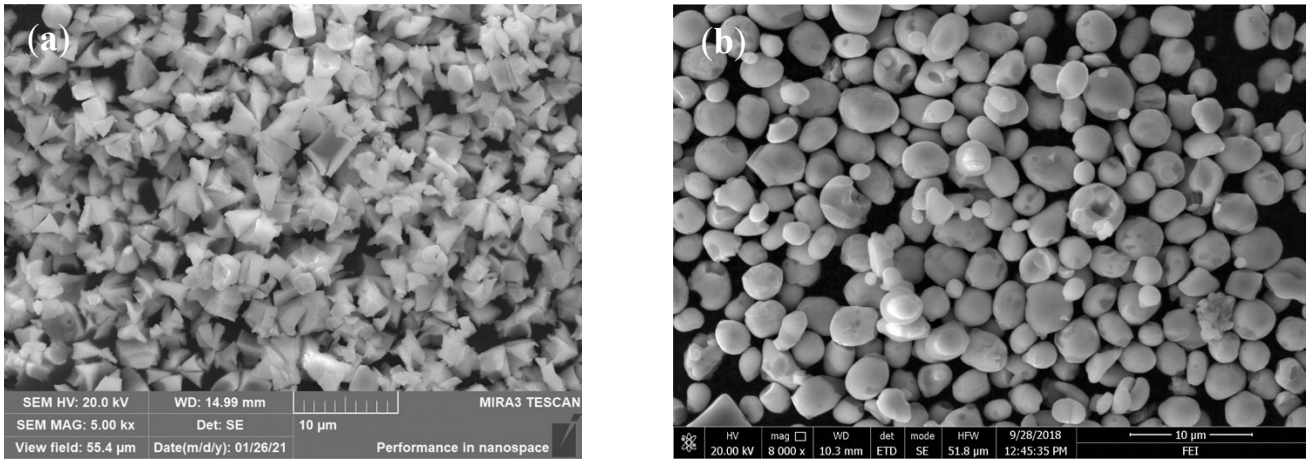


Figure 6. Three-dimensional characterization of inclusions using the inclusion extraction technique. (**a**) Without rare-earth addition; (**b**) With rare-earth addition. Reprinted with permission from Ref. [40]. Copyright 2022 Springer Nature.

Yue [41] found that adding 0.0065–0.016% rare-earth elements to 10PCuRE weathering steel modified the inclusions and significantly increased the pitting potential and pitting corrosion resistance of the rare-earth weathering steel.

Liu [42] found that the inclusions in rare-earth-treated Q460NH steel were mainly composed of $(RE)_2O_2S$–$(RE)_xS_y$. Compared with the steel matrix, this phase exhibited a lower potential, indicating that these inclusions had lower resistance to pitting corrosion than the matrix. The pitting initiation process is shown in Figure 7.

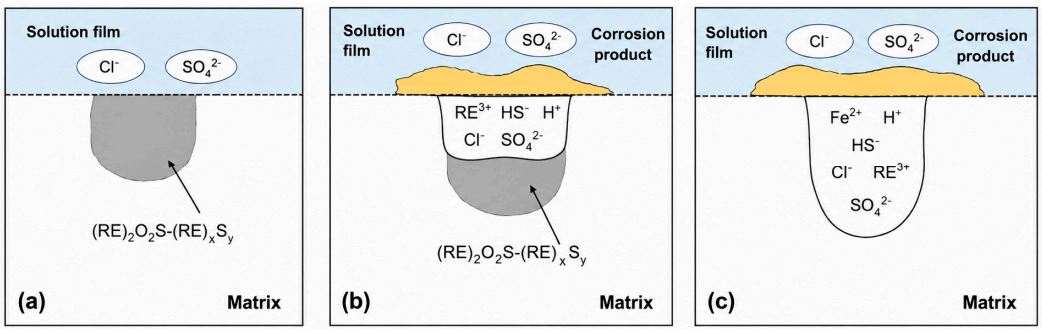


Figure 7. Initiation and propagation of pitting corrosion induced by $(RE)_2O_2S$–$(RE)_xS_y$ inclusions. (**a**) Initial stage; (**b**) Inclusion dissolution stage; (**c**) Corrosion propagation stage.

Li [40] evaluated the corrosion resistance of GCr15 bearing steel. The results showed that low-oxygen GCr15 bearing steel exhibited lower susceptibility to marine corrosion.

The substantial reduction in the number and size of inclusions modified by RE addition was the main reason for the significant improvement in the properties of the steel.

In summary, different types of inclusions induce pitting corrosion through different mechanisms. The currently recognized mechanisms of inclusion-induced pitting initiation can be classified into the following three types. First, inclusions dissolve in corrosive media and induce pitting corrosion. For example, Williams et al. found that MnS inclusions themselves dissolved in chloride-containing environments. Second, dissolution of the steel matrix surrounding inclusions induces pitting corrosion. Third, micro-galvanic couples formed between inclusions and the steel matrix induce pitting corrosion. For example, Torkkeli et al. suggested that galvanic coupling between MnS inclusions and the steel matrix was the main cause of early localized corrosion in ultra-low-carbon steel.

The addition of rare-earth elements to steel can alter the types of inclusions, transforming MnS and Al_2O_3 inclusions, which readily induce pitting corrosion, into RE_2O_3, RE_2O_2S, RE_2S_3, and $REAlO_3$ inclusions with lower pitting potentials, thereby reducing their adverse effects on steel properties. Meanwhile, the inclusions modified by rare-earth elements are smaller and more uniformly distributed, which reduces the probability of pitting corrosion and consequently improves the pitting corrosion resistance of the steel.

3.3. Effects of Rare-Earth Deoxidation and Desulfurization on Corrosion Resistance

Extensive studies have been conducted on the effect of S on the corrosion resistance of steel, mainly because sulfides formed by S can induce pitting corrosion and participate in the cathodic reactions of the corrosion process. Wilde [43] investigated austenitic stainless steel and found that high-purity sulfur-containing alloys were susceptible to attack in aqueous ferric chloride solutions, and that the severity of corrosion increased with increasing sulfur content. Gao Lixin [44] found that, under highly acidic conditions, the presence of elemental sulfur promoted the cathodic reactions of carbon steel. The addition of sulfur altered the structure of the corrosion product film, reduced its electrical resistance, and increased the corrosion rate. Liu Yichao [45] found that, at 60 °C and relative humidities of 60% and 90%, S participated in the cathodic corrosion reaction, forming FeS and causing general corrosion of sulfur-resistant steel. At 80 °C and a relative humidity of 30%, S also participated in the cathodic corrosion reaction and caused localized corrosion of sulfur-resistant steel. When the relative humidity increased to 60% and 90%, S underwent hydrolysis reactions, resulting in severe general corrosion of the sulfur-resistant steel. As shown in the Figure 8.

From 1934 to 1938, Bethlehem Steel Corporation initiated a series of outdoor corrosion tests involving hundreds of low-alloy steel compositions to determine the effects of various alloying elements and impurities on the corrosion resistance of steel [46–48]. Sulfur was found to have a particularly strong detrimental effect, while the effects of other elements are shown in Figure 9.

The effect of oxygen on weathering resistance initially increases and then decreases. Yan [49] found that, as the oxygen content in steel increased from 0.0020 wt% to 0.0200 wt%, the pitting potential gradually shifted in the positive direction, increasing by approximately 40 mV overall, and the stability of the steel matrix tended to increase, as shown in Figure 10. The corrosion rate first decreased and then increased, following a cubic-function relationship. When the oxygen content was within the range of 0.0020–0.0100 wt%, the corrosion resistance of the steel gradually increased; when the oxygen content was within the range of 0.0100–0.0200 wt%, the corrosion resistance gradually decreased.

Chen [50] suggested that, within the permissible range for continuously cast killed steel, as the degree of deoxidation of molten steel decreased and the oxygen mass fraction in the steel increased, the average corrosion rate of the steel decreased slightly, whereas its

pitting corrosion resistance increased relatively significantly. At the high-oxygen end of the variation curve, the average pitting depth was approximately 22.7% lower than that at the low-oxygen end. As shown in the Figure 10.

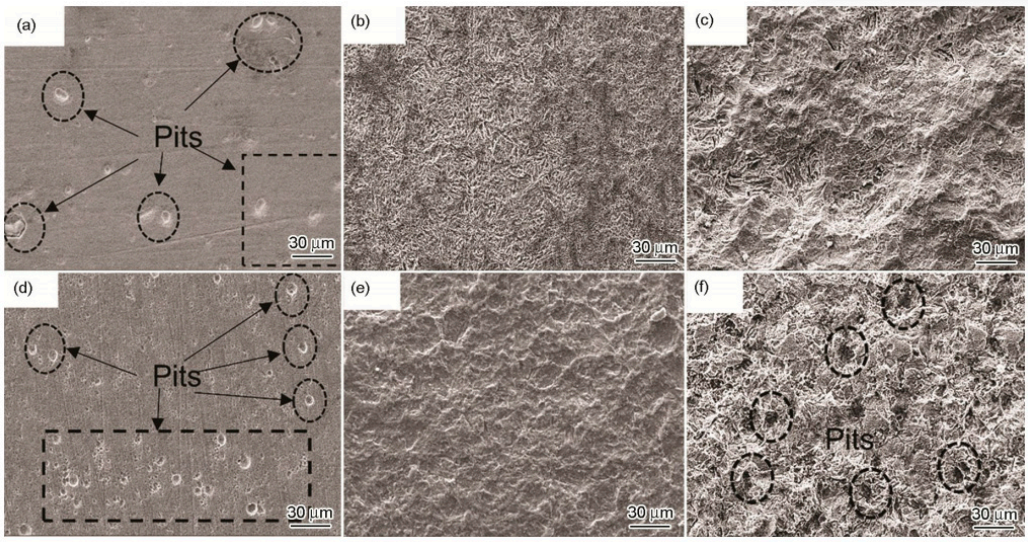


Figure 8. Surface morphology of S-covered P110SS steel after film removal at different temperatures and relative humidities. (**a**) 60 °C, 30% RH; (**b**) 60 °C, 60% RH; (**c**) 60 °C, 90% RH; (**d**) 80 °C, 30% RH; (**e**) 80 °C, 60% RH; (**f**) 80 °C, 90% RH.

It can be seen that sulfur has a detrimental effect on the corrosion resistance of steel, whereas the effect of oxygen is strongly dependent on its content. A moderate increase in oxygen content can improve corrosion resistance by promoting favorable inclusion characteristics and rust-layer evolution. However, excessive oxygen may increase the amount of oxide inclusions and introduce additional initiation sites for localized corrosion, thereby increasing the susceptibility to pitting corrosion. The addition of rare-earth elements enables the formation of compounds with sulfur and oxygen, thereby reducing the contents of free sulfur and oxygen in steel and mitigating the adverse effects of these surface-active elements on corrosion resistance. Vahed [51] found that rare-earth elements should be capable of reducing the contents of soluble oxygen and sulfur in molten steel to levels far below those currently achieved in most industrial and laboratory practices. A low sulfur content also prevents the formation of MnS inclusions.

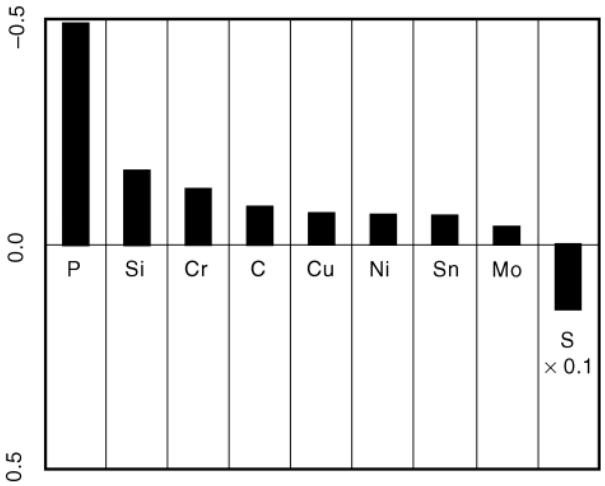


Figure 9. Effects of different elements on corrosion loss based on the average B values for the test sites (the more negative the value, the lower the corrosion loss).

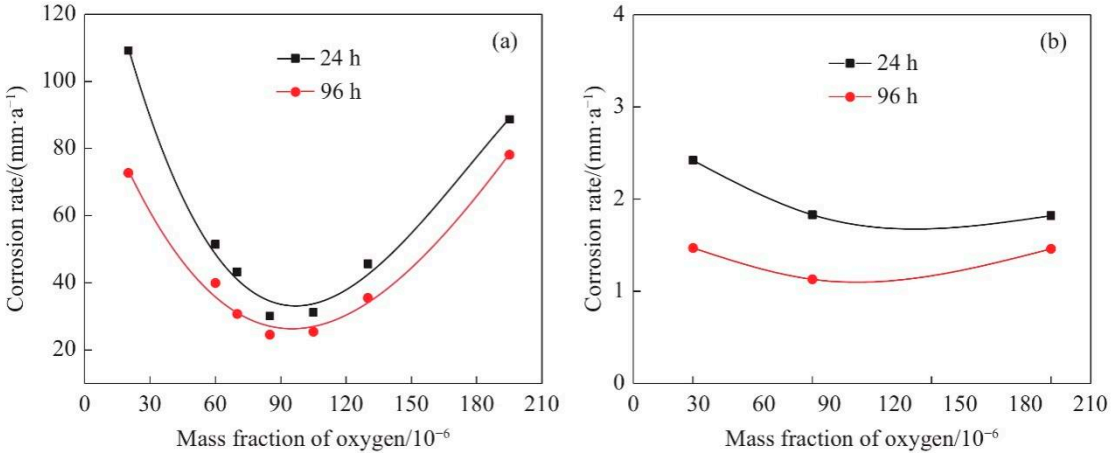


Figure 10. Effect of oxygen content on corrosion resistance. (**a**) average corrosion rate; (**b**) average pitting corrosion rate.

3.4. Effect of Rare-Earth-Induced Microstructural Refinement on Corrosion Resistance

Relatively few studies have investigated the effect of rare-earth-induced microstructural refinement on corrosion resistance, with most research focusing on the influence of grain-size refinement on mechanical properties.

Zhang [52] found that the addition of a trace amount of Ce, below 0.0020 wt%, to high-strength steel refined the grain size, reduced the grain-boundary energy, promoted the formation of rust layers containing the protective phases α-FeOOH and Fe_3O_4, increased the compactness of the rust layer, and reduced the corrosion rate. Wang [53] investigated the effects of rare-earth metals on the microstructure, mechanical properties, and pitting corrosion resistance of duplex stainless steel. The results showed that the addition of rare-earth metals led to the formation of micro-/nanoscale REM inclusions and refined the alloy microstructure. Excellent mechanical properties and pitting corrosion resistance were obtained when the REM content was within the range of 0.018–0.031 wt%, as shown in Figure 11.

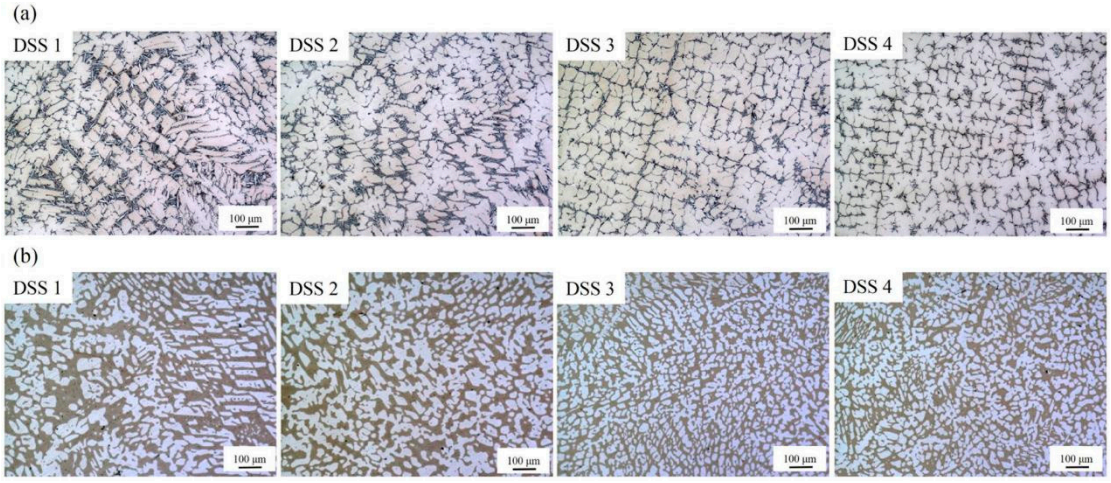


Figure 11. Microstructural evolution: (**a**) as-cast alloy; (**b**) solution-treated alloy.

Huang [54] found that the addition of rare-earth elements to high-strength steel could refine the microstructure of the material, eliminate microcracks or micropores, and prevent corrosion caused by such defects.

According to the classical Hall–Petch relationship, grain refinement can enhance the mechanical properties of materials, but it does not necessarily result in better corrosion

resistance. Nevertheless, grain refinement is highly likely to suppress defect formation, improve grain-boundary stability, and reduce grain-boundary susceptibility. Through its coupling with other factors, grain refinement can thereby improve the corrosion resistance of steel.

It should be noted that rare-earth elements do not directly replace the functions of traditional weathering elements such as Cu and Cr. Cu and Cr mainly enhance corrosion resistance through their enrichment in the inner rust layer, promotion of stable α-FeOOH formation, and reduction in ionic diffusion pathways. In comparison, rare-earth elements exert their effects through multiple routes, including molten-steel purification, inclusion modification, grain refinement, and regulation of rust-layer development. Therefore, the role of RE in low-alloy weathering steels is better described as a synergistic modification strategy rather than a direct substitution for Ni or Cr.

The optimal combination of RE with reduced Ni/Cr contents depends on steel composition, corrosion environment, and required service performance. Although RE addition provides potential for reducing the consumption of expensive alloying elements, quantitative substitution criteria remain unclear and require further systematic investigation.

4. Research on the Occurrence Forms of Rare-Earth Elements in Steel

4.1. Summary of the Evolution of Rare-Earth Inclusions

A series of studies has been conducted on the evolution of rare-earth inclusions. Wang Longmei [55–57] calculated the La–O–S equilibrium phase diagram in molten iron to predict the formation of inclusions, as shown in Figure 12. The results showed that, with increasing S content, the transformation sequence $La_2O_3 \rightarrow La_2O_2S \rightarrow La_xS_y$ occurred, whereas with increasing O content, the transformation sequence $La_xS_y \rightarrow La_2O_2S \rightarrow La_2O_3$ occurred. However, the effect of Al was not considered in the investigated system.

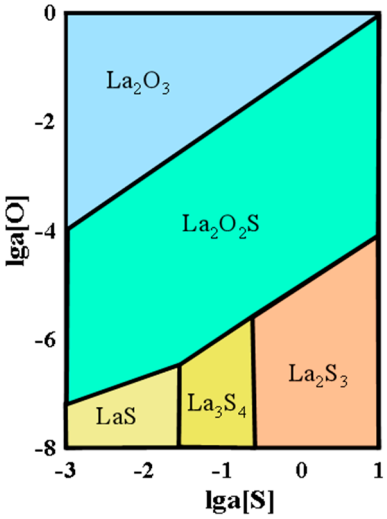


Figure 12. La–O–S equilibrium phase diagram for industrially pure iron. Thermodynamic parameters were obtained from Ref. [55].

Wang Yeguang [58] found that, as the Al mass fraction in heat-resistant steel increased within the range of 0–0.3%, the typical inclusions in the steel evolved according to the sequence $Ce_2O_3 \rightarrow Ce_2O_3 + CeAlO_3 \rightarrow CeAlO_3 + Ce_2O_2S$. Li [59] found that, with increasing La content in high-Al steel, the inclusions underwent the transformation sequence $Al_2O_3 \rightarrow LaAl_{11}O_{18} \rightarrow LaAlO_3 \rightarrow La_2O_2S \rightarrow La_2S_3$. Ren [60] suggested that, with the continuous increase in Ce content in ultra-low-carbon Al-deoxidized steel, the inclusions underwent the transformation sequence $Al_2O_3 \rightarrow CeAlO_3 \rightarrow Ce_2O_2S \rightarrow Ce_2O_2S + CeS$.

Kang [61] found that, after the addition of rare-earth elements to HRB500E steel, Al_2O_3–MnO–CaO complex inclusions were transformed into spherical or ellipsoidal $REAlO_3$ and $REAlO_3$–MnS complex inclusions, and no isolated MnS inclusions were observed. Geng [62] found that, after Ce addition, the typical inclusions in Al-deoxidized steel changed from calcium aluminate inclusions to (Ca–Ce–S–O) + (Ce–Al–Ca–O) complex inclusions.

In industrial rare-earth weathering steel production, inclusion evolution is not governed by a single RE–O–S or RE–Al reaction system, but by the coupled effects of residual deoxidizing elements and refining treatments. Aluminum, calcium, and rare-earth elements compete for oxygen and sulfur during ladle refining. For Al-killed steels, residual [Al] strongly affects inclusion evolution by promoting the formation of Al_2O_3 and RE–Al–O phases. Subsequent Ca treatment modifies alumina inclusions through calcium aluminates, while rare-earth addition can further transform these inclusions into RE-containing oxides, oxysulfides, or complex Ca–RE–Al–O–S inclusions depending on the local chemical activities.

Therefore, the evolution sequence of inclusions in industrial rare-earth steels should be considered as a multi-component thermodynamic process rather than a simple binary or ternary transformation. Although simplified phase diagrams (e.g., La–O–S and Ce–Al–O systems) provide fundamental understanding, accurate prediction of inclusion stability before casting requires coupling multicomponent thermodynamic calculations with actual refining conditions, including [Al], [Ca], [O], [S], and RE activities.

4.2. Reaction Products of Rare-Earth Elements with Impurity Elements

Research on the interactions between rare-earth elements and impurity elements originated from the work of Du Ting and Wang Longmei at the Central Iron and Steel Research Institute. They found that the addition of trace amounts of rare-earth elements to clean steel could achieve deep deoxidation, desulfurization, and dephosphorization, reduce the segregation of S and P at grain boundaries, and improve grain-boundary characteristics. Rare-earth elements could also react with harmful low-melting-point elements such as As, Sb, Bi, Pb, and Sn to form compounds with relatively high melting points, thereby suppressing the segregation of these low-melting-point elements at grain boundaries.

Wang [63,64] investigated the reaction mechanism between rare-earth elements and As and found that the La–As binary compound had a cubic structure with a lattice constant of 0.6162 nm and a chemical formula of LaAs. $LaAsO_4$ and LaAs began to form during and after solidification and tended to precipitate at grain boundaries. Thermodynamic calculations were also conducted for La–As–O–S inclusions, and the corresponding equilibrium phase diagram of the inclusions was obtained, as shown in Figure 13.

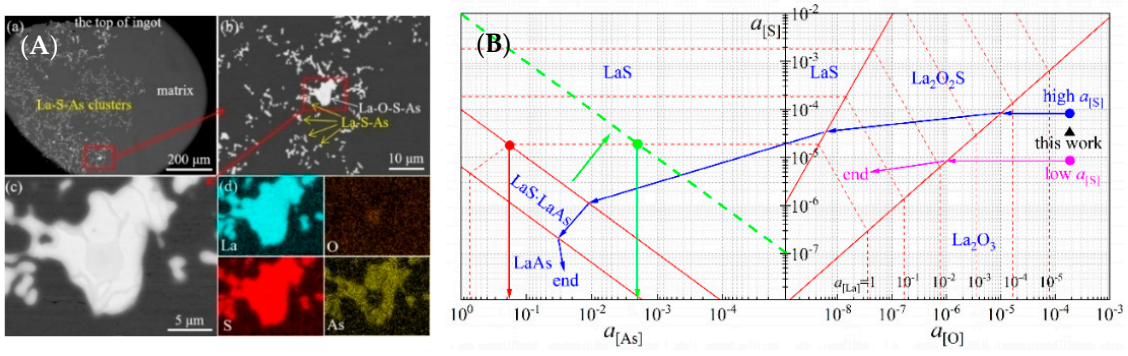


Figure 13. Rare-earth arsenides. (**A**) Morphology of rare-earth de-arsenization products; (**B**) Predominance area diagram of La–As–O–S inclusions. Reprinted from Refs. [63,64].

Taking C104Cr saw-wire steel as an example, Li [65] investigated the reaction tendencies of rare-earth elements with various elements in steel. It was found that, under the thermodynamic conditions of molten steel, the Gibbs free energy changes for the formation reactions of rare-earth arsenides, phosphides, and carbides were positive, as shown in Figure 14, indicating that these compounds were formed during solidification. The Brody–Flemings model was further used to calculate the precipitation behavior of these three types of compounds during solidification, and the results showed that all of them formed at the final stage of solidification.

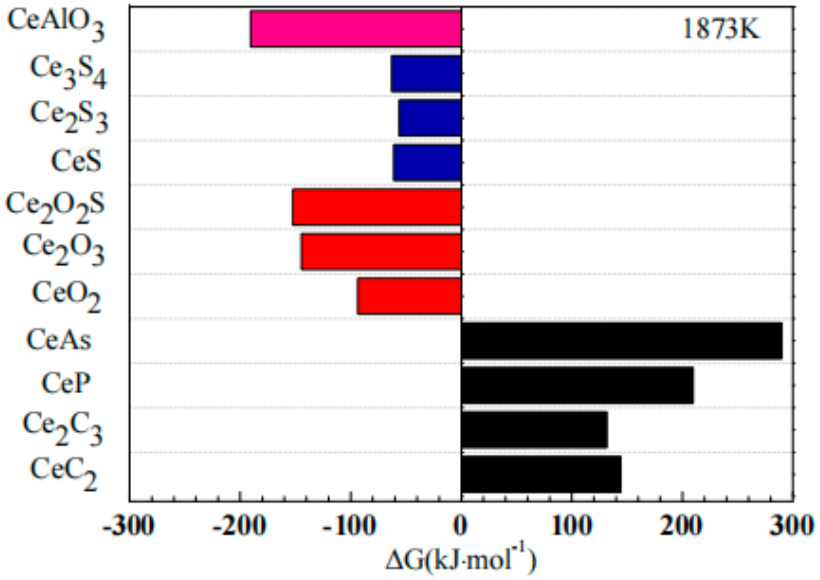


Figure 14. Gibbs free energy changes for the formation reactions of rare-earth arsenides, phosphides, and carbides. Reprinted from Ref. [65].

Studies on the removal of impurity elements by rare-earth La have mainly focused on As, and a specific reaction mechanism has been established. However, rare-earth elements can also react with N to form rare-earth nitrides, with C to form rare-earth carbides, and with H to form rare-earth hydrides, such as LaH_3 and CeH_2. The interactions of rare-earth La with C, Si, Al, P, N, Sn, Pb, and Bi still require further investigation. Meanwhile, it remains necessary to clarify whether the reaction products formed between rare-earth elements and impurity elements are primary or secondary inclusions.

4.3. Detection Methods and Evidence for Rare-Earth Elements in Solid Solution

Rare-earth elements in solid solution in metals refer to rare-earth atoms dissolved in the crystal lattice to form a solid solution. Current methods for determining the amount of rare-earth elements in solid solution mainly include [66–69]: (1) physical methods, including internal-friction measurements, positron-annihilation techniques, and lattice-parameter measurements, which are generally limited to qualitative and semiquantitative analyses; and (2) chemical methods, in which rare-earth inclusions are separated by electrolysis and the amount of rare-earth elements in solid solution is subsequently determined using different analytical methods. As shown in the Figure 15.

Many studies have used X-ray diffraction (XRD) to investigate the solid solution of rare-earth elements in steel, but the conclusions obtained are not consistent. Gao Xueyun [70] measured the XRD patterns of steels with different rare-earth contents and found that the characteristic peaks shifted to the right with increasing rare-earth content. This indicated that the Fe lattice structure was distorted and that a portion of the introduced rare-earth elements was dissolved in the Fe lattice. However, other researchers [71,72] found that

the characteristic peaks shifted to the left with increasing rare-earth content, indicating that the degree of distortion of the Fe lattice structure decreased. The reduction in the lattice parameter of Fe was mainly attributed to the reactions of Ce with O, S, Al, C, N, As, Si, and other elements, which reduced the amounts of other elements in solid solution and consequently decreased the lattice parameter of Fe. Therefore, XRD peak shifts alone cannot provide direct evidence of rare-earth solid-solution behavior. The final diffraction response depends on the relative contribution of RE substitution, impurity scavenging, and precipitation of RE-containing compounds. Advanced atomic-scale techniques, such as atom probe tomography (APT), are necessary to directly reveal the local distribution of rare-earth atoms and their interactions with interstitial elements.

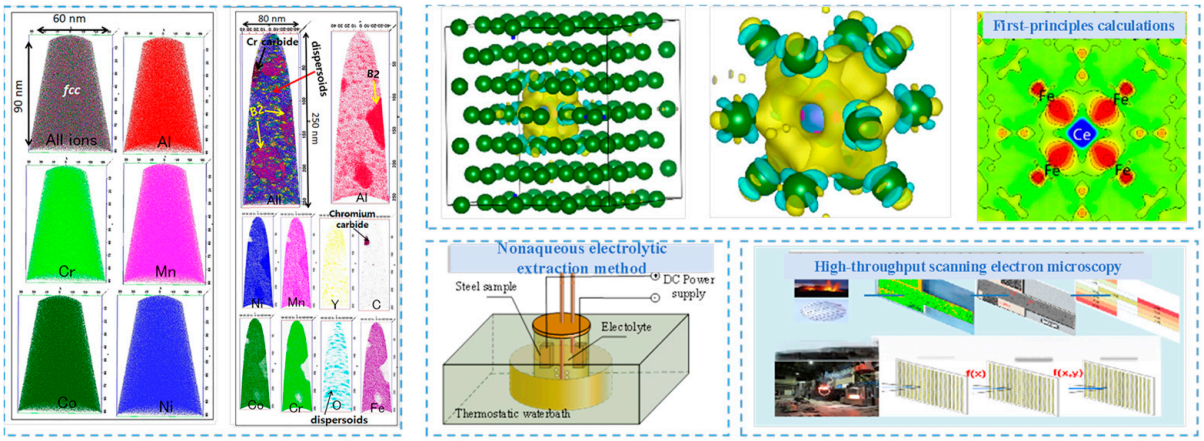


Figure 15. Common detection and analysis methods for rare-earth elements in solid solution.

In recent years, the development of high-throughput scanning electron microscopy and atom probe tomography [73,74] has made the detection of rare-earth elements in solid solution possible. However, these two methods also have certain limitations. Their observation regions are relatively small, often at the nanometre scale, making it difficult to reliably capture rare-earth elements in solid solution and resulting in a degree of randomness in the observations.

Many researchers have also conducted first-principles calculations on rare-earth elements in solid solution. Liu [75] analysed the atomic-site occupancy and solid-solution mechanism of Ce and found that Ce could substitute for Fe atoms in an α-Fe supercell. Charge transfer occurred between Ce and the surrounding Fe atoms: Ce lost electrons, while the surrounding Fe atoms gained electrons. Ionic polarization occurred between Fe and Ce, resulting in a reduction in the effective radius of Ce. This study provided a theoretical basis for the solid solution of rare-earth elements in steel.

Lin Qin et al. [76,77] investigated the amount of rare-earth elements in solid solution in 16Mn steel. In one method, X-ray fluorescence spectroscopy was used to determine the total rare-earth content in the steel and the rare-earth content in the inclusions separated by electrolysis. The difference between these two values was taken as the amount of rare-earth elements in solid solution. In another method, plasma emission spectroscopy was used to directly determine the rare-earth content in the electrolyte, and this value was regarded as the amount in solid solution. The results are shown in Figure 16a. Figure 16b presents the amount and variation in La in solid solution in low-sulfur 16Mn steel, as determined by Lin Qin et al. using the ICP method. It can be seen that, in general, the amount of rare-earth elements in solid solution in steel is relatively low, mostly below 10^{-5}.

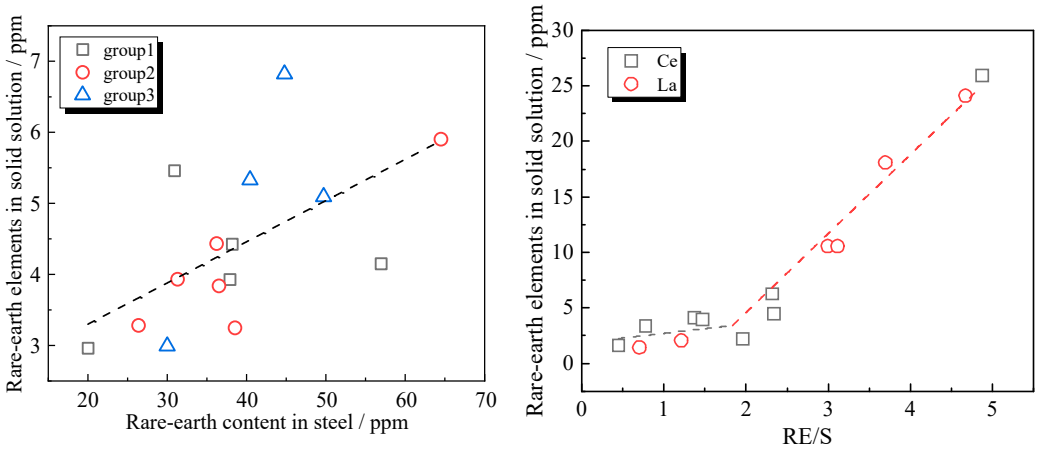


Figure 16. Relationships among the rare-earth content in steel, the RE/S ratio, and the amount of rare-earth elements in solid solution. (**a**) Effect of Ce content on the amount of rare-earth elements in solid solution; (**b**) Effect of the RE/S ratio on the amount of rare-earth elements in solid solution.

5. Research on Nozzle Clogging in Rare-Earth Steels

5.1. Types of Nozzle-Clogging Deposits in Rare-Earth Steels

The earliest literature on nozzle clogging in rare-earth steels can be traced back to the 1980s. Previous studies have mainly focused on the chemical analysis of nozzle-clogging deposits, while relatively little attention has been paid to thermodynamic analysis. Consequently, the clogging problem has not yet been fundamentally resolved. By screening, statistically summarizing, and analysing the literature on the castability of La- and Ce-containing rare-earth steels in China and abroad, the current research status of molten-steel castability in rare-earth steels was obtained, as shown in Table 3.

Table 3. Summary of literature on the castability of rare-earth steels in China and abroad [78–87].

Steel Grade	Rare-Earth Element	Nozzle Material	Composition of Clogging Deposits	Process Route	Improvement Measures
Steel for construction machinery	La + Ce	Alumina–carbon	$REAlO_3$ + RE_2O_3 + solidified steel	LD–LF–RH–CC; deoxidation with ferrosilicon, rare-earth addition before vacuum break in RH	Control the oxygen content at a low level and reduce the formation of Al_2O_3 inclusions; modify the deoxidation method; avoid alumina–carbon nozzles and use fused-silica nozzles instead.
253MA stainless steel	Ce	Alumina–carbon	RE_2O_3 + Al_2O_3–RE compounds + SiO_2–RE compounds + solidified steel	Laboratory induction-furnace experiment	Prevent secondary oxidation of molten steel, reduce the number of small inclusions in steel, and avoid reactions between molten steel and the nozzle.
16MnRE	La + Ce	Alumina–carbon	$REAlO_3$ + RE_2O_3 + RE_2O_2S + RE_2S_3 + solidified steel	LD–LF–CC; Al deoxidation; rare-earth wire feeding in the tundish	Prevent the formation of a decarburized layer or replace the nozzle with a silica-based nozzle; adopt a non-Al deoxidation process or conduct precise calcium treatment of molten steel; prevent secondary oxidation of molten steel.

Table 3. *Cont.*

Steel Grade	Rare-Earth Element	Nozzle Material	Composition of Clogging Deposits	Process Route	Improvement Measures
—	La + Ce	Alumina–carbon	Al_2O_3 + $REAlO_3$ + $CaO{\cdot}2Al_2O_3$ + solidified steel	KR–BOF–LF–RH–CC; Al deoxidation + calcium treatment + addition of rare-earth ferroaluminum alloy at the end of RH treatment	Improve the cleanliness of molten steel and rare-earth alloys; develop refractory materials specifically for nozzles; reduce the reactivity between nozzle refractories and rare-earth elements.
Bearing steel for wind turbines	Ce	Alumina–carbon	$CeAlO_3$ + Ce_2S_3 + solidified steel	Rare-earth addition in the tundish	Prevent the formation of a decarburized layer and suppress reactions between the submerged entry nozzle and inclusions.
253MA stainless steel	La + Ce	Alumina–zirconia	RE_2O_2S + RE_2O_3 + solidified steel	EAF–AOD–LF–CC; Si deoxidation; rare-earth alloy addition during LF refining	Optimize nozzle geometry, improve steel cleanliness, prevent secondary oxidation of molten steel, and reduce the amount of rare-earth compounds by removing SiO_2 inclusions and improving the flow conditions in the tundish.
253MA stainless steel	Ce	Alumina–carbon with ZrO_2–Y_2O_3 coating	$CeAlO_3$ + Ce_2O_2S + solidified steel	Laboratory induction-furnace experiment	Increase the holding time before continuous casting, apply a YSZ coating and fully preheat it in advance, and increase the Ce/Al ratio.
E36 ship-building steel	Y	Magnesia–carbon	Y_2O_3 + SiO_2 + $2Y_2O_3{\cdot}Al_2O_3$ + Y_2SiO_5 + Fe_2O_3	KR–BOF–LF–CC; calcium treatment; rare-earth wire feeding	Improve molten-steel cleanliness and reduce the Al content in molten steel or nozzle refractories.
Stainless steel	Ce	Alumina–silica with glass/silicon-powder coating	$CeAlO_3$ + Ce_2O_3 + REM silicate compounds	Laboratory electric-furnace experiment	Fully preheat the nozzle and reduce the content of basic oxides in the coating.
253MA stainless steel	La + Ce	Alumina–carbon	$REAlO_3$ + RE_2O_3	EAF–AOD–CC; Al deoxidation; calcium treatment	Reduce the amount of high-melting-point rare-earth oxides precipitated in steel, replace the nozzle material, increase the basicity of the tundish covering flux, and increase the B_2O_3 and Li_2O contents.

As can be seen from Table 3, the steel grades investigated in existing studies cover a wide range of categories, including stainless steels, weathering steels, and bearing steels. Studies conducted outside China have mainly focused on 253MA steel. As a heat-resistant austenitic stainless steel, 253MA requires high creep resistance, corrosion resistance, and strength. A small amount of rare-earth elements must be added to achieve the required oxidation resistance; therefore, rare-earth addition is indispensable for this steel grade.

China has relatively abundant rare-earth resources and has therefore developed a wider variety of rare-earth steels, including wear-resistant tool steels, shipbuilding steels, and bearing steels. Existing studies have sufficiently demonstrated the advantages of

rare-earth addition [88]. The rare-earth additions used are mainly Ce-based alloys and La–Ce alloys. Because the thermodynamic data for La-containing compounds remain incomplete, relatively few studies have been conducted on La alloying. In the periodic table, La has stronger reducing ability than Ce. However, the influence of the differences in their chemical properties on nozzle clogging has received relatively little attention.

5.2. Mechanism of Submerged Entry Nozzle Clogging

Nozzle-clogging deposits mainly consist of rare-earth deoxidation and desulfurization products and rare-earth aluminates formed in the steel. The agglomeration and adhesion of rare-earth inclusions are the main causes of clogging [88]. Rare-earth aluminates generated through reactions between rare-earth elements in molten steel and nozzle refractories have relatively low interfacial energy with rare-earth inclusions in the steel. This facilitates the adhesion and sintering of rare-earth inclusions on these reaction products, which act as a substrate and promote clogging. The nozzle-clogging mechanism is illustrated in Figure 17.

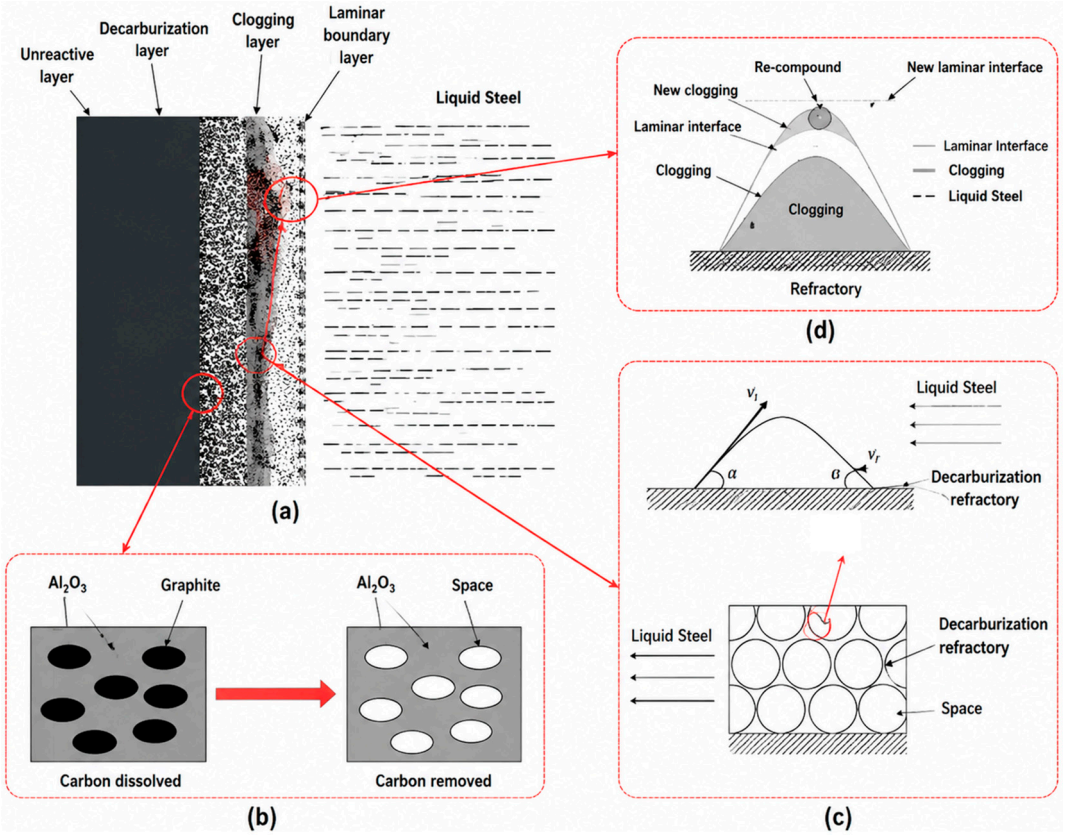


Figure 17. Schematic diagram of the nozzle-clogging mechanism. (**a**) Overall structural schematic diagram of the waterhole interface; (**b**) Decarburization mechanism of refractory materials; (**c**) Molten steel flow and inclusion adhesion mechanism at the decarburization layer interface; (**d**) Continuous growth mechanism of slag inclusions.

As shown in the figure, nozzle clogging occurs through the following steps:

- Sufficient reaction time: Immediately adjacent to the nozzle surface, the flow velocity of molten steel approaches zero, forming a viscous boundary layer.
- Formation of a substrate for clogging deposits: Rare-earth elements in molten steel react with the nozzle material to form rare-earth compounds.
- Adhesion and sintering on the rare-earth-compound substrate: High-melting-point rare-earth inclusions carried by the molten steel move at very low velocities within the boundary layer and adhere to and sinter on the rare-earth-compound substrate.

- Continued adhesion and sintering of rare-earth inclusions: The deposits grow in dendritic and network-like forms, dividing the molten steel flow and increasing the contact area with the steel, thereby promoting the continued adhesion of large quantities of inclusions from the molten steel.
- Complete nozzle blockage: Owing to the large temperature gradient, the molten steel is divided into fine streams. Some portions are trapped by inclusions and solidify, whereas others adhere to the outside of the nozzle and form solidified-steel accretions. These accretions further enhance heat dissipation and accelerate the development of clogging.

After rare-earth elements are added to molten steel in the ladle, accretions often form at the nozzle or runner, causing nozzle clogging. The morphology of the accretions is shown in Figure 18.

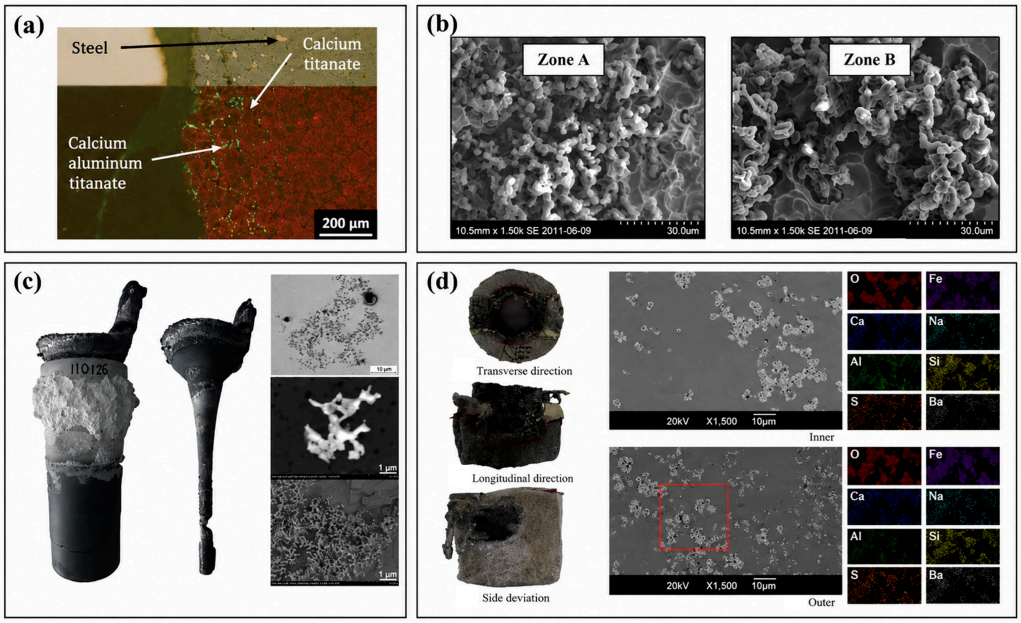


Figure 18. Images of nozzle clogging deposits. (**a**) Cross-sectional view; (**b**) three-dimensional original morphology of the clogging deposit; (**c**) photograph of the clogging deposit; (**d**) clogging deposit.

Metallurgical researchers have generally recognized that improving molten-steel cleanliness and changing the nozzle material and final deoxidizer can significantly help prevent nozzle clogging. For rare-earth-treated steels, to reduce the clogging caused by rare-earth addition, optimal metallurgical thermodynamic conditions must be provided before and during rare-earth addition:

- The oxygen and sulfur contents in the molten steel should be maintained at the lowest possible levels.
- Appropriate stirring should be applied during rare-earth addition to ensure the uniform distribution of rare-earth elements.
- Protective casting should be adopted to strictly prevent secondary oxidation of the molten steel.
- Pure rare-earth metal wire or high-purity mischmetal wire must be properly protected to minimize the oxidation and burning loss of the rare-earth wire.
- An appropriate rare-earth addition amount must be determined according to the cleanliness and performance requirements of each steel grade.

5.3. Anti-Clogging Technologies for Submerged Entry Nozzles

Nozzle clogging has long been a persistent problem in the production of high-quality steels. To address this issue, researchers in China and abroad have conducted extensive studies and industrial practices [89–101] and have adopted corresponding measures under different conditions, effectively reducing the occurrence of nozzle clogging.

(1) Optimization of process conditions. Calcium treatment is applied to modify high-melting-point inclusions in Al-killed and Al–Si-killed steels, thereby promoting the formation of low-melting-point complex inclusions and preventing the deposition of high-melting-point inclusions on the inner wall of the nozzle. However, the application of this measure is limited in non-calcium-treated steel grades, such as bearing steels. Meanwhile, argon sealing should be strengthened to prevent the secondary oxidation of molten steel. The preheating temperature of the submerged entry nozzle should also be increased, and the thermal insulation conditions should be improved. These measures can alleviate nozzle clogging to a certain extent.

(2) Development of anti-clogging coatings for the inner wall of nozzles. From the perspective of materials, the properties of the inner-wall material are optimized to alter its wettability with molten steel, inhibit reactions among molten steel, inclusions, and the nozzle wall, reduce the tendency of inclusions to deposit, and improve the smoothness of the inner surface. For this purpose, various lining materials have been developed, including ZrO_2–CaO–C, carbon-free spinel, corundum, Al_2O_3–SiO_2, MgO–SiO_2–CaO, and $CaTiO_3$ materials. Different lining materials suppress clogging through different mechanisms. In addition, their anti-clogging performance is closely related to the specific application environment and operating conditions.

(3) Novel submerged entry nozzle structures. The molten-steel flow field inside the nozzle is optimized by generating vortices in the nozzle bore and outlet ports and by applying intense stirring or other measures. These approaches suppress the residence of inclusions on the inner wall of the nozzle and thereby inhibit accretion formation. Parabolic-bottom nozzles, swirl nozzles driven by electromagnetic forces or guide vanes, stepped nozzles, and Mogul nozzles are representative anti-clogging nozzles developed through structural innovation, as shown in Figure 19.

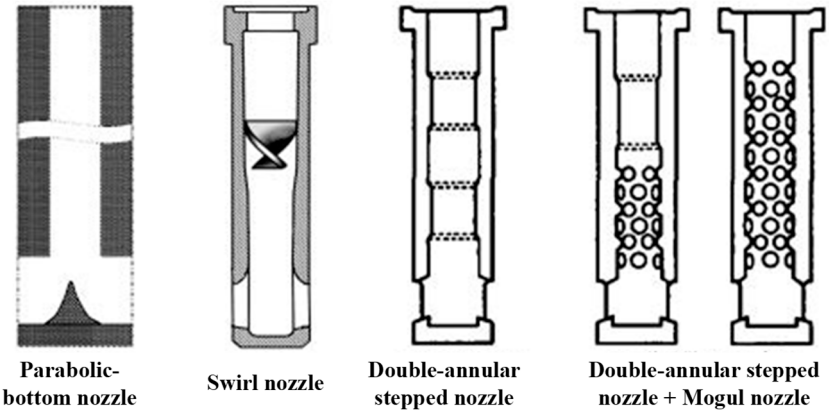


Figure 19. Anti-clogging submerged entry nozzles with different structural designs.

(4) Application of Physical Fields. In addition, methods such as the use of stopper rods, argon injection through the nozzle, and externally applied electromagnetic fields can also alleviate nozzle clogging. Argon injection can form an argon-gas film on the inner wall of the nozzle, increase the turbulence intensity of the molten steel, and prevent inclusions from depositing on the inner surface. Moreover, because the nozzle is under negative pressure during casting, argon injection can reduce the pressure drop within the nozzle and limit

the ingress of oxygen from the surroundings, thereby helping to alleviate the secondary oxidation of molten steel. However, during this process, argon bubbles may become entrapped in the cast product, resulting in product-quality problems. Argon injection may also intensify fluctuations of the liquid level in the mould, increase the probability of slag entrainment, and deteriorate the service conditions of the refractory materials.

The application of an electromagnetic field at the nozzle can cause inclusions to move in a specific direction and reduce their tendency to migrate toward the nozzle wall, thereby decreasing nozzle clogging. However, because the space beneath the tundish is very limited, practical operation is relatively difficult.

The studies described above have mainly focused on the effects of molten-steel flow dynamics, chemical factors, and other variables on refractory materials and structures, as well as on the migration and adhesion of inclusion particles. Although researchers in China and abroad have investigated the interactions between refractory materials and inclusions from multiple perspectives using various methods, no consensus has yet been reached regarding their effects and regulation. Problems such as the service failure of nozzles and the adsorption of inclusions by refractory materials have not yet been effectively resolved.

6. Research on Rare-Earth Alloying Processes

Since the 1960s, with the continuous development of steelmaking and continuous casting technologies, methods and process technologies for adding rare-earth elements to steel have undergone several stages of evolution. According to the location at which rare-earth elements are introduced, these methods can be classified chronologically as follows: direct addition into the ladle → plunging addition into the ladle → rare-earth powder injection into the ladle → rare-earth wire feeding into the ladle → suspension addition in the ingot mold → rare-earth powder injection through the trumpet → rare-earth wire feeding through the trumpet → rare-earth wire feeding into the tundish → rare-earth wire feeding into the continuous-casting mold.

Based on industrial production experience, the basic principles of the major rare-earth addition processes are illustrated in Figure 20. As shown in the figure, rare-earth addition has progressively shifted from direct addition, plunging, and powder injection in the ladle to powder injection through the trumpet, suspension addition in the ingot mold, and wire feeding into the continuous-casting mold. Consequently, rare-earth elements have tended to be introduced at increasingly later stages of the steelmaking and casting process. Different addition methods were adopted during different periods, and the principal rare-earth addition methods are summarized in Table 4.

At present, various steel plants have carried out a series of industrial trials on rare-earth alloying and applied these processes to different steel grades. The corresponding process requirements and addition stages are summarized in Table 5. Statistical analysis of rare-earth yields shows that the results vary considerably among different steel grades. In addition, the alloying methods are highly diverse, and no unified technical specification has yet been established. Because the requirements for molten-steel composition and process routes also differ, there is an urgent need to formulate systematic guidelines and standardized procedures for the production of rare-earth microalloyed steels.

As shown in Table 5, the rare-earth recovery rate varies considerably among different addition methods because of differences in their application conditions. According to industrial data, Ansteel currently employs the ladle plunging method, with a rare-earth recovery rate of 20–30%; the process used by TISCO achieves a recovery rate of approximately 40%; and the rare-earth alloying process adopted by Baogang achieves a recovery rate of about 51%. Overall, however, the recovery rates of rare-earth elements remain relatively low.

Table 4. Main Types of Rare-Earth Addition Processes [102–122].

Process Type	Steel Grade	Yield/%	Main Advantages	Existing Problems
Rare-earth plunging addition into the ladle	16Mn steel	20–25	Simple operation; uniform distribution; no nozzle clogging	Low rare-earth yield; incomplete inclusion modification
Rare-earth powder injection into the ladle	16MnRE/Y08RE	45–60	Significant reduction in [S] and [O] contents in steel	Complex equipment and cumbersome operation
Rare-earth wire feeding into the ladle	No. 20 steel	10–25	Simple operation; purification of molten steel; smooth process operation	Low rare-earth yield; incomplete inclusion modification
Rare-earth wire feeding into the tundish during continuous casting	No. 20 steel	50–75	Convenient operation; uniform distribution; high rare-earth yield; complete inclusion modification	Complex process; nozzle clogging; sintering of the tundish covering flux
Rare-earth wire feeding into the continuous-casting mold	0.9MnRE/16MnRE/08Al	70–90	Smooth process operation; high rare-earth yield; uniform distribution; complete inclusion modification	Residual inclusions; interfacial enrichment; surface defects

Under modern metallurgical conditions, rare-earth steels are generally produced through continuous casting. From the perspective of industrial feasibility, rare-earth wire feeding into the ladle is considered one of the most suitable addition methods. However, with the development of standardized and high-purity rare-earth alloys, significant progress has been achieved in the precise control of alloy composition, enhancement of alloy density, substantial reduction of oxygen, nitrogen, and sulfur contents, minimization of other impurity elements, production of alloy lumps with specified dimensions, and extension of storage life. These developments have created favorable conditions for adding rare earths to molten steel in the form of lump alloys directly charged into the ladle. Considering the uniform distribution of rare-earth elements and their effectiveness in improving steel properties, rare-earth alloying in the ladle is expected to become the predominant development direction in the future.

Table 5. Rare-Earth Alloying Processes and Recovery Rates [123–127].

Steel Grade	RE Addition Amount	Composition Requirements	Addition Timing/Method	RE Recovery Rate	Remarks
30CrNi2MoVA	0.10–0.15 kg/t steel (0.010–0.015 wt%)	Al: 0.01–0.05 wt%; S ≤ 0.006 wt%; O ≤ 0.0020 wt%	Rare earths are added immediately after vacuum release at the end of VD treatment, followed by soft Ar stirring for 5–10 min; the total soft-stirring time is 30–50 min.	≥50%	—
GCr15 bearing steel (Shandong Steel)	$(10–200) \times 10^{-6}$ (0.001–0.020 wt%)	$T[O] \leq 10 \times 10^{-6}$; $[S] \leq 30 \times 10^{-6}$	Ar gas at 0.2–1.5 MPa is used as the carrier gas to inject rare earths into the molten steel through an injection lance. The insertion depth is approximately one-third to two-thirds of the bath depth, with feeding performed from the top.	—	Lump rare-earth alloy is used, with an equivalent diameter of 5–40 mm and a length-to-width or axial-to-width ratio of 1–3.
Anhui Fukai	25 kg/heat	$T[O] \leq 100 \times 10^{-4}$ wt%; [S] ≤ 0.010 wt%; tapping temperature: 1640 °C	The alloy is added during AOD tapping. A Ce alloy with a purity of 65% is polished before use and placed at the bottom of the ladle using a dedicated charging bucket.	62–71%	A dedicated charging bucket is used.

Table 5. *Cont.*

Steel Grade	RE Addition Amount	Composition Requirements	Addition Timing/Method	RE Recovery Rate	Remarks
Corrosion-resistant reinforcing steel	11.2 kg for 7 t of steel	[O] < 0.0040 wt%	The rare-earth alloy is placed in the empty ladle 5–10 min after the addition of the deoxidizing alloy, followed by the addition of the other alloying elements.	85%	A self-prepared sintered alloy containing 5–20 wt% RE is used, with slag carryover below 5 kg/t steel.
Rare-earth structural steel (Baotou Steel)	0.01 wt% mixed rare-earth alloy	[O] < 0.0004 wt%	After rare-earth addition, vacuum circulation is continued for 3 min before terminating the vacuum treatment.	35–50%	The rare-earth alloy contains 30 wt% RE, with Ce/La = 2:1.
Cr12 cold-work die steel	Added in two batches, 0.05–0.075 kg/t steel per batch	Al: 0.01–0.05 wt%; S ≤ 0.005 wt%; O ≤ 0.0020 wt%	Rare earths are first added after deoxidation and alloying are completed during LF refining, and then added again immediately after vacuum release from VD treatment. Soft Ar stirring is maintained for 30–50 min after vacuum release, followed by tapping and ingot casting.	≥50%	After LF refining, the SiO_2 content in the slag is controlled at ≤10%. A dedicated plunging rod is used for addition.
Rare-earth microalloyed steel (Baotou Steel)	(10–200) × 10^{-6} (0.001–0.020 wt%)	Al: 0.030–0.050 wt%	After Ca treatment, soft Ar stirring is maintained for at least 5 min. Rare earths are added 15 min after the start of vacuum treatment, approximately 5 min before vacuum release. Pure degassing is continued for at least 8 min after addition, and the combined soft-stirring and holding time is at least 15 min.	—	The LF slag basicity is controlled at 4.5–7.5. After vacuum release, [H] ≤ 0.00012 wt%, [O] ≤ 0.0020 wt%, and [N] ≤ 0.0040 wt%.
EH36	80 kg of Si–Mg–RE alloy containing 3.16 wt% RE; 8 kg of pure rare-earth metal with a purity of 99.99 wt%	S: 0.0020 wt%; Als: 0.038 wt%; measured dissolved oxygen: 0.00023 wt%	The RH vacuum-treatment time is 15 min, including 11 min of pure degassing. At 2 min before vacuum release, 80 kg of Si–Mg–RE alloy is added. Immediately after Ca-wire feeding, 8 kg of sealed pure rare-earth metal is added, followed by soft Ar stirring for 10 min.	58%	Pure rare-earth metal is used, with Ce/La = 2:1.
High-purity rare-earth steel (Baotou Steel)	40 kg of Nd-, La-, or Ce-containing rare-earth material	O ≤ 0.0010 wt%; C ≤ 0.0010 wt%; S ≤ 0.0010 wt%; [O + C + S] ≤ 0.0020 wt%	After 4–5 min of pure degassing during RH treatment, the circulation-gas flow rate is adjusted to 1000–1400 NL/min and rare earths are added. Vacuum release is performed after a further 7–8 min of pure degassing. Casting begins after holding for 11–12 min following vacuum release.	20–25%	No nozzle clogging occurs under this treatment method.
High-strength reinforcing steel (Central Iron and Steel Research Institute)	One or more rare-earth elements selected from La, Ce, and Y	O/S < 0.20; RE/S = 1.6–2.2	Rare earths are introduced in the form of a cored wire fed directly into the continuous-casting mold. The diameter of the RE cored wire is 3–15 mm.	80–90%	The cored wire contains 10–50 wt% RE and 10–20 wt% Si, with RE/(Ca + Mg) = 10–100.
Rare-earth bearing steel (Shijiazhuang Steel)	The final RE content is controlled at ≤0.020 wt%, with a deviation of no more than 0.0020 wt%.	S ≤ 0.002 wt%; Ca ≤ 0.0004 wt%; FeO in slag ≤ 0.25 wt%	One-stage Al deoxidation is adopted without Ca treatment. Rare-earth alloying is conducted using a dedicated addition device. After alloying, soft Ar stirring is maintained for 5–7 min to ensure uniform mixing, followed by high-vacuum treatment at ≤67 Pa for 28–30 min before vacuum release.	—	Rare earths are added using a dedicated addition device equipped with a charging bucket.

Table 5. *Cont.*

Steel Grade	RE Addition Amount	Composition Requirements	Addition Timing/Method	RE Recovery Rate	Remarks
Rare-earth steel (Northeastern University)	—	—	Rare-earth powder with a particle size below 45 μm is injected through the bottom of the tundish. The powder quantity is determined according to the molten-steel mass and injected using Ar gas.	>75%	A dedicated powder-injection device is used.

The research team led by Li Dianzhong at the Institute of Metal Research, Chinese Academy of Sciences, developed the "dual-low-oxygen rare-earth steel" technology [40]. This technology involves the simultaneous control of low oxygen in molten steel, with the total oxygen content reduced to T.O < 0.0020 wt%, and low oxygen in rare-earth metals, with T.O < 0.0060 wt%, La + Ce ≥ 99 wt%, and Ce/La ≈ 2. This approach effectively addresses key bottlenecks restricting the industrial application of rare-earth steels. When applied to high-cleanliness GCr15 bearing steel, the tension–compression fatigue life under ±800 MPa was increased by a factor of 40 and the rolling-contact fatigue life was improved by 40% compared with bearing steel without rare-earth addition. In contrast, the fatigue life of samples treated with conventional commercial rare-earth metal containing 0.027 wt% oxygen exhibited pronounced fluctuations, as shown in Figure 21.

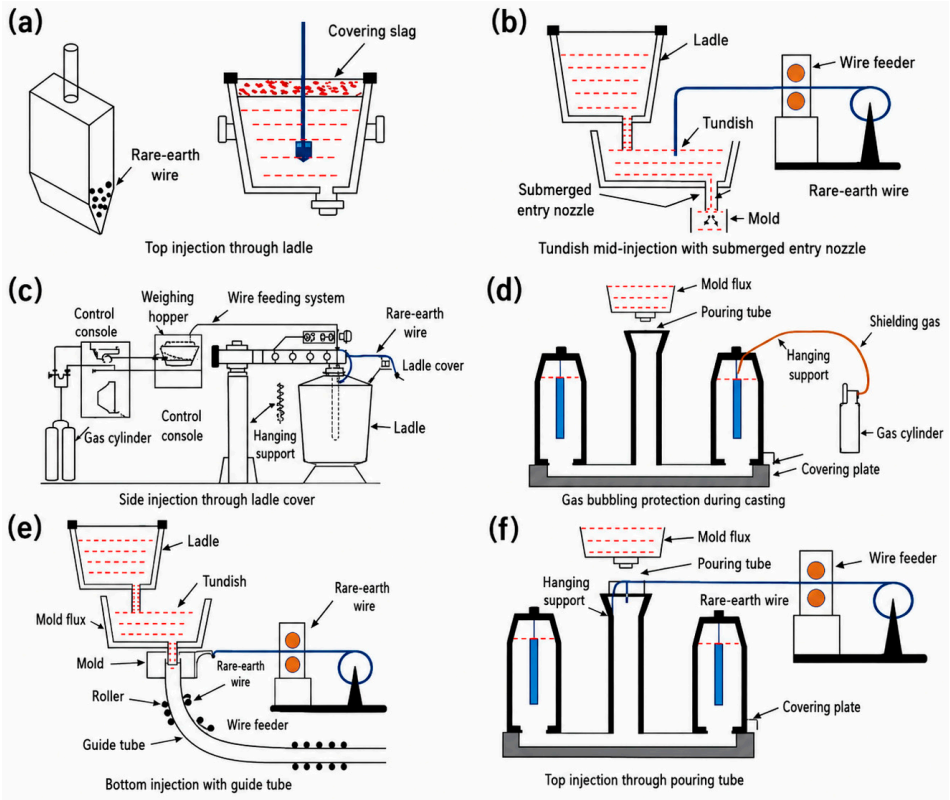


Figure 20. Schematic diagram of the principal rare-earth addition processes. (**a**) Rare-earth addition into the ladle; (**b**) Rare-earth wire feeding into the tundish during continuous casting; (**c**) Rare-earth powder injection into the ladle; (**d**) Suspension addition in the ingot mold during ingot casting; (**e**) Rare-earth wire feeding into the continuous-casting mold; (**f**) Rare-earth wire feeding through the trumpet during ingot casting.

Dual-low-oxygen rare-earth steel not only effectively reduces the number and size of inclusions and improves their characteristics, thereby alleviating nozzle clogging during

continuous casting, but also provides favorable conditions for the dissolution of rare-earth elements in the steel matrix, making it possible for them to exert a microalloying effect. This study revealed that oxygen is the fundamental factor responsible for fluctuations in the properties of rare-earth steels. Only under low-oxygen conditions can rare-earth elements consistently refine and modify inclusions and exert a pronounced microalloying effect.

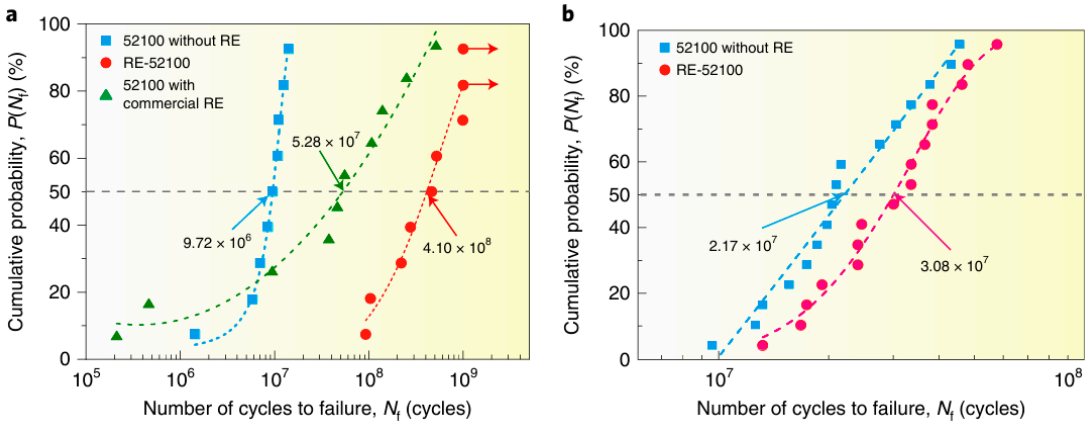


Figure 21. The superior effects of re addition on the tensile–compression and rolling contact fatigue lives of 52,100 steels. (**a**) The influence of rare earth elements on the tensile and compressive fatigue life of 52,100 steel; (**b**) The influence of rare earth elements on the rolling contact fatigue life of 52,100 steel. Reprinted with permission from Ref. [40]. Copyright 2022 Springer Nature.

The results further demonstrate that the addition of only several hundred grams of light rare-earth elements, such as La and Ce, per tonne of steel can significantly improve steel properties with almost no increase in production cost and without substantial modification of the existing process route. This is of considerable significance for exploiting China's rare-earth resource advantages, promoting the balanced utilization of rare-earth resources, and improving the quality of high-grade special steels.

Although the dual-low-oxygen strategy was originally proposed for bearing steels requiring extremely high cleanliness, its application in structural weathering steels should be optimized according to steel grade requirements. For weathering steels, moderately controlled oxygen levels combined with low sulfur conditions may provide a practical balance between stable rare-earth modification and industrial production cost.

7. Conclusions

(1) The corrosion resistance of weathering steel is mainly affected by the rust layer structure, alloy composition, inclusion characteristics and microstructure. Among them, the dense and stable inner rust layer can effectively prevent the further penetration of the corrosive medium into the steel matrix, and the formation of stable corrosion products such as α-FeOOH is particularly critical for improving corrosion resistance. Alloying elements such as Cu, P, Cr and Ni can promote the formation of protective rust layer and enhance its stability. In recent years, due to the high cost of Ni and Cr and the limitation of resource supply, the weathering steel with reduced Ni and Cr addition has gradually become an important development direction.

(2) Rare earth elements can improve the corrosion behavior of weathering steel through a variety of mechanisms. On the one hand, the rare earth elements dissolved in the matrix or segregated at a specific position can regulate the electrochemical reaction process on the steel surface and promote the formation of a denser and more stable rust layer; on the other hand, rare earth can also refine the microstructure, improve the grain boundary characteristics, and reduce the tendency of local corrosion. Under the condition of reasonable control

of the addition amount, only a small amount of rare earth can play the above role, which provides a new technical way to improve the corrosion resistance of weathering steel and reduce the amount of traditional alloying elements.

(3) The type and distribution of inclusions are important factors governing the pitting behavior of weathering steel. Inclusions such as MnS, CaS, Al_2O_3, and $MgAl_2O_4$ can readily act as pitting initiation sites. Rare-earth treatment can modify these inclusions into rare-earth-containing phases such as RE_2O_3, RE_2O_2S, RE_2S_3, and $REAlO_3$, while reducing their size and promoting a more dispersed distribution. Consequently, the probability of pitting initiation is reduced, and the resistance of the steel to localized corrosion is improved.

(4) The occurrence state of rare-earth elements in steel directly determines their effectiveness. The contents of O, S, Al, and Ca in steel affect the formation and transformation of rare-earth inclusions, resulting in their evolution among oxides, oxysulfides, sulfides, and rare-earth aluminates. When molten-steel cleanliness is insufficient, rare-earth elements preferentially react with O and S, leading to a reduced rare-earth recovery rate and making it difficult to retain rare earths stably in solid solution. Therefore, the control of low-oxygen and low-sulfur clean steel, together with the regulation of rare-earth occurrence states, is fundamental to achieving stable performance in rare-earth weathering steels.

(5) The industrial production of rare-earth weathering steel still faces challenges associated with fluctuations in rare-earth recovery and insufficient castability during continuous casting. High-melting-point inclusions, including rare-earth oxides, sulfides, oxysulfides, and rare-earth aluminates, can readily adhere to, sinter on, and accumulate along the inner wall of the submerged entry nozzle, resulting in nozzle clogging and, in severe cases, complete blockage. These problems reduce the number of consecutively cast heats and impair production efficiency. Therefore, the large-scale application of rare-earth weathering steel requires coordinated optimization of the rare-earth addition stage, molten-steel cleanliness, protective casting, nozzle material, and inclusion control, so as to establish a stable and controllable rare-earth alloying process.

Funding: This research was funded by the Youth Science Foundation Project of the Natural Science Foundation of Inner Mongolia Autonomous Region, grant number 2025QN05129, and the Independent Research Projects of Central Iron and Steel Research Institute Co., Ltd., grant numbers 24160770Z and 23160360ZD.

Data Availability Statement: No new data were created or analyzed in this study. Data sharing is not applicable to this article.

Conflicts of Interest: Author Libin Yang was employed by the company Central Iron and Steel Research Institute Co., Ltd. The remaining authors declare that the research was conducted in the absence of any commercial or financial relationships that could be construed as a potential conflict of interest.

References

1. Morcillo, M.; Díaz, I.; Cano, H.; Chico, B.; de la Fuente, D. Atmospheric corrosion of weathering steels: Overview for engineers. Part I: Basic concepts. *Constr. Build. Mater.* **2019**, *213*, 723–737. [CrossRef]
2. Smith, G. Steels fit for the countryside. *New Sci.* **1971**, *52*, 211–213.
3. *ASTM A709/A709M-03*; Standard Specification for Carbon and High-Strength Low-Alloy Structural Steel Shapes, Plates, and Bars and Quenched-and-Tempered Alloy Structural Steel Plates for Bridges. ASTM International: West Conshohocken, PA, USA, 2004.
4. Wilson, A.D. Properties of recent production of A709 HPS-70W bridge steels. In *International Symposium on Steel for Fabricated Structures*; ASM International: Cincinnati, OH, USA, 1999; p. 41.
5. Zhang, W.Z.; Xu, Z.S. Research and application status of fire-resistant weathering steel. *New Build. Mater.* **2004**, *3*, 62–64. (In Chinese)
6. Dong, H.; Lian, X.T.; Hu, C.D.; Lu, H.C.; Peng, W.; Zhao, H.S.; Xu, D.X. Progress in theories and technologies for high-performance steels. *Acta Metall. Sin.* **2020**, *56*, 25–29. (In Chinese)

7. Han, C.; Li, Z.; Yang, X.; Wang, J. Corrosion behavior and mechanical performance of weathering steel in industrial and rural atmospheric environments. *Constr. Build. Mater.* **2024**, *411*, 134284. [CrossRef]
8. Du, C.-C.; Qin, M.-H.; Wu, Z.-F.; Li, D.-L.; Zhao, L.; Li, X.-Y.; Wang, H.-Z. Multi–performance evaluation of high–throughput accelerated corrosion test for high-strength low-alloy 921A steel. *J. Iron Steel Res. Int.* **2023**, *31*, 1260–1278. [CrossRef]
9. Xia, F.; Li, J.; Wu, Q.; Zhao, Y.; Wang, J.; Su, X.; Peng, H.; Li, Z. Exploring the influence of Cu addition on the microstructure and substance transformation in corrosion product layer of X80 steel. *Mater. Charact.* **2023**, *207*, 113589. [CrossRef]
10. Wang, B.; Liu, Q.Y.; Mao, X.P.; Weng, Y.; Wang, X.D.; Jia, S.J.; Dong, H. Effect of RE (Rare Earth) on the corrosion resistance of carbon steel in 0.3 mol/L NaCl solution. *Acta Metall. Sin.* **2008**, *44*, 863–866.
11. Liu, Y.; Guo, K.; Cui, W.; Ma, Y.; Zhang, J.; Yu, Q. Unraveling the Corrosion Mechanism and Electrochemical Properties of the Rust Layer for Weathering Steel with Different SO42-Concentrations in the Simulated Atmosphere. *J. Mater. Eng. Perform.* **2026**, *35*, 21702–21716. [CrossRef]
12. Zhang, Q.C.; Wu, J.S.; Chen, J.G. Analysis of the rust layer on atmospheric-corrosion-resistant steel after one-year exposure. *J. Chin. Soc. Corros. Prot.* **2001**, *5*, 42–45. (In Chinese)
13. Liu, X.; Yang, C.; Ma, Z.; Yang, J.; Ren, H.; Zhang, X.; Zhao, Z. Mechanisms of pitting induced by containing Ce inclusions in X100 pipeline steel. *J. Mater. Res. Technol.* **2024**, *33*, 8631–8643. [CrossRef]
14. Huang, X.; Qiu, W.; Niu, B.; Zou, X.; Pan, L.; Kwok, C.T. Role of complex nonmetallic inclusions on the localized corrosion resistance of wire arc additively manufactured super duplex stainless steel. *J. Mater. Res. Technol.* **2023**, *28*, 799–813. [CrossRef]
15. Gao, R.; Wang, L.; Wang, F.; Yang, S.; Liu, C.; Chen, C.; Li, J.; Li, X. Insights into local corrosion induced by inclusions and thermodynamic stability of inclusions in oil–casing steel by zirconium treatment. *Corros. Sci.* **2023**, *227*, 111737. [CrossRef]
16. Zhang, L.; Yu, Y.; Mao, W.; Zhang, J.; Chang, C.; Zhang, S.; Yan, W. Revealing the effect of Ce on pitting corrosion induced by inclusions in low alloy steel: Induction by $CaS{\cdot}C_{12}A_7$ and inhibition by $CeAlO_3$. *Langmuir* **2024**, *40*, 25193–25206. [CrossRef]
17. Liang, Y.-Y.; Ni, P.-Y.; Li, Y.; Chiu, Y.-L. Effect of Rare Earth Metal Alloying on Pitting Corrosion Resistance and Corrosion Layer Formation of High-Strength Oil Casing Steels. *Metall. Mater. Trans. B* **2025**, *56*, 6652–6667. [CrossRef]
18. Park, I.J.; Lee, S.M.; Kang, M.; Lee, S.; Lee, Y.K. Pitting corrosion behavior in advanced high strength steels. *J. Alloys Compd.* **2015**, *619*, 205–210. [CrossRef]
19. Zhang, B.; Wang, J.; Wu, B.; Zhou, Y.; Ma, X. Quasi–in–situ ex–polarized TEM observation on dissolution of MnS inclusions and metastable pitting of austenitic stainless steel. *Corros. Sci.* **2015**, *100*, 295–305. [CrossRef]
20. Du, C.; Qin, M.; Wu, Z.; Li, D.; Zhao, L.; Li, X.; Wang, H. Atmospheric corrosion behavior of 921A and Q450NQR1 weathering steels under simulated marine environment. *Int. J. Electrochem. Sci.* **2024**, *19*, 100755.
21. Hao, L.; Zhang, S.; Dong, J.; Ke, W. Atmospheric corrosion resistance of MnCuP weathering steel in simulated environments. *Corros. Sci.* **2011**, *53*, 4187–4192. [CrossRef]
22. Chen, Y.Y.; Tzeng, H.J.; Wei, L.I.; Wang, L.H.; Oung, J.C.; Shih, H.C. Corrosion resistance and mechanical properties of low-alloy steels under atmospheric conditions. *Corros. Sci.* **2005**, *47*, 1001–1021. [CrossRef]
23. Albrecht, P.; Hall, T.T., Jr. Atmospheric corrosion resistance of structural steels. *J. Mater. Civ. Eng.* **2003**, *15*, 2–24. [CrossRef]
24. Gan, L.; Lei, Y.; Jiang, Y.; Siyasiya, C.W.; Tang, Z. Effects of phosphorus on the corrosion characteristics of weathering steel in industrial environments. *J. Mater. Sci.* **2025**, *60*, 19116–19144. [CrossRef]
25. Hao, L.; Zhang, S.; Dong, J.; Ke, W. Evolution of corrosion of MnCuP weathering steel submitted to wet/dry cyclic tests in a simulated coastal atmosphere. *Corros. Sci.* **2012**, *58*, 175–180. [CrossRef]
26. Chenghui, Y.; Xin, Z.; Shuliu, W.; Junhang, C.; Hao, Z.; Qiang, Y.; Kui, X. Corrosion behavior and mechanism of Cr and Cu alloy weathering steel in simulated marine atmospheric environment. *J. Mater. Res. Technol.* **2025**, *35*, 3098–3106. [CrossRef]
27. Yamashita, M.; Miyuki, H.; Matsuda, Y.; Nagano, H.; Misawa, T. The long-term growth of the protective rust layer formed on weathering steel by atmospheric corrosion during a quarter of a century. *Corros. Sci.* **1994**, *36*, 283–299. [CrossRef]
28. Yamashita, M.; Shimizu, T.; Konishi, H.; Mizuki, J.; Uchida, H. Structure and protective performance of atmospheric corrosion product of Fe–Cr alloy film analyzed by Mössbauer spectroscopy and with synchrotron radiation X–rays. *Corros. Sci.* **2003**, *45*, 381–394. [CrossRef]
29. Sun, M.; Du, C.; Liu, Z.; Liu, C.; Li, X.; Wu, Y. Fundamental understanding on the effect of Cr on corrosion resistance of weathering steel in simulated tropical marine atmosphere. *Corros. Sci.* **2021**, *186*, 109427. [CrossRef]
30. Fan, Z.; Xi, Z.; Liu, T.; Lian, X.; Wei, X.; Dong, H. Study of effects of rare earth elements on the corrosion behavior of weathering steels under a simulated immersion environment and a real atmospheric environment. *Mater. Corros.* **2024**, *75*, 1539–1548. [CrossRef]
31. Chen, X.; Dong, J.; Han, E.; Ke, W. Effect of Ni on the ion–selectivity of rust layer on low alloy steel. *Mater. Lett.* **2007**, *61*, 4050–4053. [CrossRef]
32. Nishimura, T.; Katayama, H.; Noda, K.; Kodama, T. Effect of Co and Ni on the corrosion behavior of low alloy steels in wet/dry environments. *Corros. Sci.* **2000**, *42*, 1611–1621. [CrossRef]

33. Zhang, S.; Liu, J.; Tang, M.; Zhang, X.; Wu, K. Role of rare earth elements on the improvement of corrosion resistance of microalloyed steels in 3.5 wt% NaCl solution. *J. Mater. Res. Technol.* **2021**, *11*, 519–534. [CrossRef]
34. Zhu, Y.H.; Zhuang, J.; Yu, Y.S.; Zeng, X. Research on the anticorrosion property of a rare-earth inhibitor for X70 steel. *J. Rare Earths* **2013**, *31*, 734–740. [CrossRef]
35. Lian, X.; Zhu, J.; Wang, R.; Liu, T.; Xu, J.; Xu, D.; Dong, H. Effects of rare earth (Ce and La) on steel corrosion behaviors under wet–dry cycle immersion conditions. *Metals* **2020**, *10*, 1174. [CrossRef]
36. Dong, R.; Li, H.; Zhang, X.; Deng, X.; Cui, Q.; Chen, J.; Yang, X.; Liang, J. Influence of lanthanum on the corrosion resistance of steel plate for offshore platforms. *Mater. Res. Express* **2021**, *8*, 096526. [CrossRef]
37. Jia, Y.; Zhou, C.; Gao, Y.; Zhou, Y.; Liu, M.; Wang, H. Atmospheric corrosion resistance of weathering angle steels in a simulated industrial atmosphere. *J. Mater. Eng. Perform.* **2020**, *29*, 1225–1234. [CrossRef]
38. Niu, G.; Yuan, R.; Misra, R.D.K.; Gong, N.; Zhang, Z.-H.; Chen, H.-X.; Wu, H.-B.; Shang, C.-J.; Mao, X.-P. Effect of La on the Corrosion Behavior and Mechanism of 3Ni Weathering Steel in a Simulated Marine Atmospheric Environment. *Acta Metall. Sin.* **2023**, *37*, 308–324. [CrossRef]
39. Xu, H.; Guo, L.; Hu, J.; Chen, L.; Han, Y.; Lu, B.; Zhao, H.; Bai, J.; Wei, X.; Dong, H. In–situ studies of rust layer formed on OCTG N80 steels alloyed with rare earth elements. *J. Mater. Res. Technol.* **2024**, *28*, 2280–2289. [CrossRef]
40. Li, D.; Wang, P.; Chen, X.-Q.; Fu, P.; Luan, Y.; Hu, X.; Liu, H.; Sun, M.; Chen, Y.; Cao, Y.; et al. Low–oxygen rare earth steels. *Nat. Mater.* **2022**, *21*, 1137–1143. [CrossRef]
41. Yue, L.J.; Wang, L.M.; Hu, J.S. Effects of rare earths on inclusions and corrosion resistance of 10PCuRE weathering steel. *J. Rare Earths* **2010**, *28*, 952–956. [CrossRef]
42. Liu, C.; Revilla, R.I.; Liu, Z.; Zhang, D.; Li, X.; Terryn, H. Effect of inclusions modified by rare earth elements (Ce, La) on localized marine corrosion in Q460NH weathering steel. *Corros. Sci.* **2017**, *129*, 82–90. [CrossRef]
43. Williams, D.E.; Kilburn, M.R.; Cliff, J.; Waterhouse, G.I. Composition changes around sulfide inclusions in stainless steels and implications for the initiation of pitting corrosion. *Corros. Sci.* **2010**, *52*, 3702–3716. [CrossRef]
44. Gao, L.X.; Gu, T.; Yan, J.; Yu, H.L.; Liu, Z.D.; Mo, L. Effect of elemental sulfur on carbon-steel corrosion under highly acidic conditions. *Nat. Gas Ind.* **2015**, *35*, 94–98. (In Chinese)
45. Liu, Y.C.; Zhong, X.K.; Hu, J.Y. Characteristics and mechanism of elemental-sulfur corrosion of sulfur-resistant steel in wet-gas environments. *J. Chin. Soc. Corros. Prot.* **2022**, *42*, 9. (In Chinese)
46. Torkkeli, J.; Saukkonen, T.; Hänninen, H. Effect of MnS inclusion dissolution on carbon steel stress corrosion cracking in fuel–grade ethanol. *Corros. Sci.* **2015**, *96*, 14–22. [CrossRef]
47. Wilde, B.E.; Armijo, J.S. Influence of sulfur on the corrosion resistance of austenitic stainless steel. *Corrosion* **1967**, *23*, 208–214. [CrossRef]
48. Townsend, H. Effects of alloying elements on the corrosion of steel in industrial atmospheres. *Corrosion* **2001**, *57*, 497–501. [CrossRef]
49. Yan, C.; Qin, H.; Cui, G.; Qi, Q.; Zhao, M.; Liu, K. Effect of oxygen content on the corrosion resistance of steel. *Chin. J. Eng.* **2024**, *46*, 704–714. (In Chinese)
50. Chen, X.Q.; Zhang, W.L.; Chen, S.; Liu, J.-R.; Cao, G.-L.; Li, G.-M. Role of oxygen in economical corrosion-resistant steel. *Chin. J. Eng.* **2021**, *43*, 960–965. (In Chinese)
51. Vahed, A.; Kay, D.A.R. Thermodynamics of rare earths in steelmaking. *Metall. Trans. B* **1976**, *7*, 375–383. [CrossRef]
52. Xiaoyu, Z.; Ruifeng, D.; Bo, G.; Jiquan, C.; Zhipeng, M.; Weizhe, Z.; Xiong, Y. Effect of trace rare earth elements (Ce) on corrosion resistance of high strength steel used for offshore platform. *Mater. Res. Express* **2023**, *10*, 036514. [CrossRef]
53. Wang, H.; Wang, A.; Li, C.; Yu, X.; Xie, J.; Liang, T.; Liu, C. Effects of rare earth metals on microstructure, mechanical properties, and pitting corrosion of 27% Cr hyper duplex stainless steel. *Rev. Adv. Mater. Sci.* **2022**, *61*, 873–887. [CrossRef]
54. Huang, Y.; Jin, X.; Cai, G. Evolution of microstructure and mechanical properties of a new high strength steel containing Ce element. *J. Mater. Res.* **2017**, *32*, 3894–3903. [CrossRef]
55. Wu, Y.; Wang, L.; Du, T. Thermodynamics of rare earth elements in liquid iron. *J. Less Common Met.* **1985**, *110*, 187–193. [CrossRef]
56. Wang, L.; Du, T.; Yue, K. A Study of thermodynamics and phase equilibria in order to predict the behavior of yttrium in iron and steel. *Inorganica Chim. Acta* **1987**, *140*, 189–191. [CrossRef]
57. Wang, L.; Du, X.; Gan, Y.; Liu, L.; Ye, X. Effect of rare earths on the oxidation resistance of heat-resistant steel. *J. Rare Earths* **2010**, *28*, 489–491. [CrossRef]
58. Wang, Y.G.; Liu, C.J.; Qiu, J.Y. Effect of aluminum on nonmetallic inclusions in rare-earth heat-resistant steel. *Iron Steel* **2022**, *57*, 52–57. (In Chinese)
59. Li, B.; Zhu, H.; Zhao, J.; Song, M.; Li, J.; Xue, Z. Effect of Rare-Earth La on Inclusion Evolution in High-Al Steel. *Steel Res. Int.* **2022**, *93*, 2100347. [CrossRef]
60. Ren, Q.; Zhang, L. Effect of cerium content on inclusions in an ultra-low-carbon aluminum-killed steel. *Metall. Mater. Trans. B* **2020**, *51*, 589. [CrossRef]

61. Kang, J.; Yu, Y.-C.; Zhang, J.-L.; Chen, C.; Wang, S.-B. Effect of rare earth on inclusion evolution in industrial production of HRB500E steel. *Metall. Res. Technol.* **2021**, *118*, 220. [CrossRef]
62. Geng, R.; Li, J.; Shi, C. Evolution of inclusions with Ce addition and Ca treatment in Al-killed steel during RH refining process. *ISIJ Int.* **2021**, *61*, 1506–1513. [CrossRef]
63. Wang, H.; Jiang, S.; Yu, P.; Bai, B.; Sun, L.; Wang, Y. Distribution of arSENic inclusions in rare earth steel ingots. *Metals* **2020**, *10*, 146. [CrossRef]
64. Wang, H.; Yu, P.; Jiang, S.; Bai, B.; Sun, L.; Wang, Y. Evolution of inclusions in steelmaking process of rare earth steels containing arSENic with alumina crucibles. *Metals* **2020**, *10*, 275. [CrossRef]
65. Li, Y.; Sun, M.; Jiang, Z.; Chen, C.; Chen, K.; Huang, X.; Sun, S.; Li, H. Inclusion modification in C104Cr saw wire steel with different cerium content. *Metals* **2019**, *9*, 54. [CrossRef]
66. Ji, J.W. Internal-friction study of rare-earth alloying in iron and steel. *Physics* **1993**, *22*, 4. (In Chinese)
67. Fang, K.M.; Ni, R.M.; Li, B.S. Electrolytic separation of rare-earth inclusions in steel. *Iron Steel* **1985**, 21–27. (In Chinese)
68. Song, Y.F.; Luo, W. Determination of the total amount of rare-earth inclusions in low-alloy steel. *Baosteel Technol.* **1994**, *5*. (In Chinese)
69. Gao, X.; Wang, H.; Xing, L.; Ma, C.; Ren, H. Evolution of local atomic structure during solidification of an Fe–RE (RE = La, Ce) alloy. *J. Non-Cryst. Solids* **2020**, *542*, 120109. [CrossRef]
70. Wang, H.; Gao, X.; Ren, H.; Chen, S.; Yao, Z. Diffusion coefficients of rare-earth elements in fcc Fe: A first-principles study. *J. Phys. Chem. Solids* **2018**, *112*, 153–157. [CrossRef]
71. Wang, L.M.; Lin, Q.; Yue, L.J.; Liu, L.; Guo, F.; Wang, F.M. Study of application of rare earth elements in advanced low alloy steels. *J. Alloys Compd.* **2008**, *451*, 534–537. [CrossRef]
72. Jingsheng, Y.; Zongsen, Y.; Chengjian, W. Rare earths and the mechanical properties of steel. *JOM* **1988**, *40*, 26–31. [CrossRef]
73. Zhang, W.Y.; Ren, Q.; Wang, H.; Wan, W.H.; Wang, H.Z. Research progress in high-throughput experimentation and characterization techniques for materials. *China Sci.* **2023**, *18*. (In Chinese)
74. Liu, J.; Xu, L.; Shi, C.; Yang, S.; He, X.; Wang, M.; Shi, J. Effect of rare-earth Ce on sulfide characteristics and microstructure in non-quenched and tempered steel. *Acta Metall. Sin.* **2021**, *58*, 365–374. (In Chinese)
75. Liu, X.J. Occurrence State of Rare-Earth Ce in Steel and Its Mechanisms Affecting Mechanical and Corrosion Properties. Ph.D. Thesis, Inner Mongolia University of Science and Technology, Baotou, China, 2021. (In Chinese) [CrossRef]
76. Lin, Q.; Guo, F.; Zhu, X.Y. Grain-boundary behavior of lanthanum and cerium in clean C–Mn steel. *J. Chin. Soc. Rare Earths* **2006**. (In Chinese) [CrossRef]
77. Lin, Q.; Guo, F.; Zhang, L.M.; Gao, P.X.; Wang, Y.H.; Zhao, C.R. Alloying effect of lanthanum in clean C–Mn steel. *Chin. Rare Earths* **2005**, *26*, 37–41. (In Chinese) [CrossRef]
78. Li, Z.C.; Xu, S.H.; Xu, T.; Han, H.T.; Wang, J.C.; Liu, Z.K. Industrial practice of adding rare-earth ferroalloy in an RH furnace. *Baotou Steel Sci. Technol.* **2019**, *45*, 14–17. (In Chinese)
79. Kojola, N.; Ekerot, S.; Andersson, M.; Jönsson, P.G. Pilot-plant study of nozzle-clogging mechanisms during casting of REM-treated stainless steels. *Ironmak. Steelmak.* **2011**, *38*, 1–11.
80. Li, Y.D. Fundamental Study on Inclusion-Behavior Control in Rare-Earth Heat-Resistant Steel. Ph.D. Thesis, Northeastern University, Shenyang, China, 2016. (In Chinese)
81. Yang, F.; Zhang, Y.S. Process control for rare-earth steelmaking and mechanism of nozzle clogging. *Baotou Steel Sci. Technol.* **2019**, *45*, 27–32. (In Chinese)
82. Tian, C.; Yu, J.K.; Jin, E.D.; Wen, T.; Jia, D.; Liu, Z.; Yuan, L. Effect of interfacial reaction behavior on the clogging of SENs in the continuous casting of bearing steel containing rare-earth elements. *J. Alloys Compd.* **2019**, *792*, 1–7. [CrossRef]
83. Zhou, S.C. Study of submerged-nozzle clogging during continuous casting of RE-253MA stainless steel. *Metallurgist* **2013**, *57*. [CrossRef]
84. Svensson, J.K.S.; Larsson, F.; Memarpour, A.; Ekerot, S.; Brabie, V.; Jönsson, P.G. Implementation of a YSZ coating material to prevent clogging of the submerged entry nozzle (SEN) during continuous casting of Ce-treated steels. *Ironmak. Steelmak.* **2018**, *45*, 105–113. [CrossRef]
85. Wen, L.; Lai, C.B.; Luo, D.Q.; Wang, X.L.; Sun, L.F.; Cao, R.H. Mechanism of tundish-nozzle clogging in yttrium-based rare-earth steel. *Jiangxi Metall.* **2019**, *39*, 10–14, 33. (In Chinese)
86. Memarpour, A.; Brabie, V.; Jönsson, P.G. Effect of glass/silicon-powder coatings on the clogging behavior of submerged entry nozzles during casting of REM-alloyed stainless steels. *Ironmak. Steelmak.* **2011**, *38*, 229–239.
87. Liu, W.D.; Liu, M.S. Research and practice on the smelting process of rare-earth-containing heat-resistant stainless steel 253MA. *TISCO Sci. Technol.* **2019**, *3*, 18–23. (In Chinese)
88. Zhu, J.; Huang, H.Y.; Xie, J.X. Recent progress in rare-earth steel research and new approaches for accelerated development. *J. Iron Steel Res.* **2017**, *29*, 513–529. (In Chinese)

89. Yang, W.; Zhang, L.; Ren, Y.; Chen, W.; Liu, F. Formation and prevention of nozzle clogging during the continuous casting of steels: A review. *ISIJ Int.* **2024**, *64*, 1–20. [CrossRef]
90. Deng, Z.; Zhu, M.; Zhong, B.; Sichen, D. Attachment of liquid calcium aluminate inclusions on inner wall of submerged entry nozzle during continuous casting of calcium–treated steel. *ISIJ Int.* **2014**, *54*, 2813–2820. [CrossRef]
91. Tsujino, R.; Tanaka, A.; Imamura, A.; Takahashi, D.; Mizoguchi, S. Mechanism of deposition of inclusions and metal in a ZrO_2–CaO–C immersion nozzle for continuous casting. *ISIJ Int.* **1994**, *34*, 853–858. [CrossRef]
92. Ma, F.X.; Gu, Q.; Liu, G.Q.; Zhang, Y.; Li, H.X. A systematic study of carbon-free oxide-based lining for preventing submerged entry nozzle clogging in continuous casting of rare earth steel. *J. Iron Steel Res. Int.* **2025**, *32*, 1584–1595. [CrossRef]
93. Chen, K.; Yuan, L.; Gu, Q.; Liu, G.; Yu, J.; Li, H. Insights into clogging behavior of Al_2O_3-C and ZrO_2-C submerged entry nozzle during continuous casting of ultra-low carbon steel. *Corros. Sci.* **2025**, *246*, 112777. [CrossRef]
94. Prasad, B.; Sahu, J.K.; Tiwari, J.N. Design and development of anti-clogging nozzles for casting aluminum-killed steel. In *Proceedings of UNITECR 2007*; The German Refractories Association (GRA): Dresden, Germany, 2007; pp. 208–211.
95. Kachi, T.; Takahashi, S.; Yamauchi, C. Development of low-adhesion materials for submerged entry nozzles used in continuous casting. *Taikabutsu* **2018**, *70*, 269–275. (In Japanese)
96. Svensson, J.K.S.; Memarpour, A.; Ekerot, S.; Brabie, V.; Jönsson, P.G. Studies of new coating materials to prevent clogging of submerged entry nozzle (SEN) during continuous casting of Al killed low carbon steels. *Ironmak. Steelmak.* **2017**, *44*, 117–127. [CrossRef]
97. Chen, K.; Wang, D.; Yuan, L.; Gu, Q.; Liu, G.; Li, H. A novel method for suppressing clogging of nozzle and stopper rod by electric current pulse during continuous casting of ultra-low carbon steel. *J. Manuf. Process.* **2025**, *151*, 1–23. [CrossRef]
98. Tsukaguchi, Y.; Hayashi, H.; Kurimoto, H.; Yokoya, S.; Marukawa, K.; Tanaka, T. Development of swirling–flow submerged entry nozzles for slab casting. *ISIJ Int.* **2010**, *50*, 721–729. [CrossRef]
99. Qiu, Z.; Cheng, Z.; Wang, Y.; Guo, M.; Blanpain, B. A transient model for submerged entry nozzle clogging: A coupled CFD and DEM approach. *Powder Technol.* **2025**, *453*, 120647. [CrossRef]
100. Osamu, N.; Shinsuke, I.; Masanori, O. Water-model simulation of a "mogul-lined" submerged entry nozzle. *Taikabutsu Overseas* **2004**, *24*, 194–197.
101. Yang, Y.; Jönsson, P.G.; Ersson, M.; Nakajima, K. Inclusion behavior under a swirl flow in a submerged entry nozzle and mold. *Steel Res. Int.* **2015**, *86*, 341–360. [CrossRef]
102. Li, C.L. Application of rare earths in steel and issues requiring attention. *Chin. Rare Earths* **2001**, *22*, 1–6. (In Chinese)
103. Zhou, L.J.; Guo, X.Y.; Dong, S.F.; He, X.P. Research and application of rare-earth addition technologies in steel. *Shandong Metall.* **2004**, *26*, 40–43. (In Chinese)
104. Wang, L.M. Roles and application prospects of rare-earth elements in a new generation of high-strength and high-toughness steels. *J. Chin. Soc. Rare Earths* **2004**, *22*, 48–54. (In Chinese)
105. Waudby, P.E. Rare earth additions to steel. *Int. Met. Rev.* **1978**, *23*, 74–98. [CrossRef]
106. Lin, Q.; Song, B.; Guo, X.M.; Zhang, M. Microalloying effects and application prospects of rare earths in steel. *Chin. Rare Earths* **2001**, *22*, 31–36. (In Chinese)
107. Jonšta, P.; Jonšta, Z.; Brožová, S.; Ingaldi, M.; Pietraszek, J.; Klimecka-Tatar, D. The effect of rare earth metals alloying on the internal quality of industrially produced heavy steel forgings. *Materials* **2021**, *14*, 5160. [CrossRef]
108. Kippenhan, N.; Gschneidner, K.A., Jr. *Rare-Earth Metals in Steels*; Iowa State University, Rare-Earth Information Center: Ames, IA, USA, 1970.
109. He, J.C. Selection of rare-earth addition processes for rare-earth microalloyed steels. *Baotou Steel Sci. Technol.* **2017**, *43*, 1–3. (In Chinese)
110. Zhao, T.Y.; Li, W.L.; Kelebek, S.; Choi, Y.; Wu, C.Q.; Zhang, W.J.; Wang, C.Y.; Zhao, Z.W.; Sadri, F. A comprehensive review on rare earth elements: Resources, technologies, applications, and prospects. *Rare Met.* **2025**, *44*, 7011–7040. [CrossRef]
111. Wu, C.C. Process and Theoretical Study of Rare-Earth Alloying During Special-Steel Refining. Ph.D. Thesis, University of Science and Technology Beijing, Beijing, China, 2015. (In Chinese)
112. Smirnov, L.A.; Rovnushkin, V.A.; Oryshchenko, A.S.; Kalinin, G.Y.; Milyuts, V.G. Modification of steel and alloys with rare-earth elements. Part 1. *Metallurgist* **2016**, *59*, 1053–1061. [CrossRef]
113. Petryna, D.Y.; Kozak, O.L.; Shulyar, B.R.; Petryna, Y.D.; Hredil, M.I. Influence of alloying by rare-earth metals on the mechanical properties of 17G1S pipe steel. *Mater. Sci.* **2013**, *48*, 575–581. [CrossRef]
114. Ma, X.; An, Z.; Chen, L.; Mao, T.; Wang, J.; Long, H.; Hongyan, X. The effect of rare earth alloying on the hot workability of duplex stainless steel—A study using processing map. *Mater. Des.* **2015**, *86*, 848–854. [CrossRef]
115. Chen, S.; Ye, H.; Lin, X. Effect of rare earth and alloying elements on the thermal conductivity of austenitic medium manganese steel. *Int. J. Miner. Metall. Mater.* **2017**, *24*, 670–674. [CrossRef]
116. Raman, A. Uses of Rare Earth Metals and Alloys in Metallurgy: Part I. Applications in Ferrous Materials. *Int. J. Mater. Res.* **1976**, *67*, 780–789.

117. Zhao, B.; Wu, W.; Zhi, J.G.; Su, S.C.; Wang, C.Y. Thermodynamic analysis for improving the castability of La- and Ce-containing molten steel. *Chin. Rare Earths* **2023**, *44*, 72–86. (In Chinese)
118. Zhao, B.; Wu, W.; Yang, F.; Zeng, J.; Liang, Z.; He, J. Effect of Cerium Element on Non-metallic Inclusions Formation During Molten and Solidification Processes of Q355 Microalloy Structural Steel. *Metall. Mater. Trans. B* **2024**, *55*, 1244–1260. [CrossRef]
119. Zhao, B.; Qiao, T.; Wu, W.; Zhi, J. Thermodynamic calculation of component activities in the CaO–CaF_2–SiO_2–Al_2O_3 quaternary slag system for crankshaft steel. *China Metall.* **2022**, *32*, 49–57. (In Chinese)
120. Zhao, B.; Wu, W.; Zhi, J.; Su, C.; Yao, T. Effect of CeO_2 Content on Melting Performance and Microstructure of CaO–Al_2O_3–SiO_2–MgO Refining Slag. *Metals* **2023**, *13*, 179. [CrossRef]
121. Zhao, B.; Wu, W.; Zhi, J.; Su, C.; Zhang, J. Formation mechanism of the clogging layer in the submerged entry nozzle during continuous casting of rare-earth-microalloyed Q355 steel and process optimization. *Ironmak. Steelmak.* **2023**, *50*, 782–793.
122. Han, Y.; Liu, Z.H.; Wu, C.B.; Zhao, Y.; Zu, G.Q.; Zhu, W.W.; Ran, X. A short review on the role of alloying elements in duplex stainless steels. *Tungsten* **2023**, *5*, 419–439. [CrossRef]
123. Tuttle, R. Effect of rare earth additions on grain refinement of plain carbon steels. *Int. J. Met.* **2012**, *6*, 51–65. [CrossRef]
124. Chu, R.; Fan, Y.; Li, Z.; Liu, J.; Yin, N.; Hao, N. Study on the control of rare earth metals and their behaviors in the industrial practical production of Q420q structural bridge steel plate. *Metals* **2018**, *8*, 240. [CrossRef]
125. Song, M.M.; Song, B.; Xin, W.B.; Sun, G.L.; Song, G.Y.; Hu, C.L. Effects of rare earth addition on microstructure of C–Mn steel. *Ironmak. Steelmak.* **2015**, *42*, 594–599. [CrossRef]
126. Preinfalk, C.; Morteani, G. The industrial applications of rare-earth elements. In *Lanthanides, Tantalum and Niobium: Mineralogy, Geochemistry, Characteristics of Primary Ore Deposits, Prospecting, Processing and Applications*; Springer: Berlin, Germany, 1989; pp. 359–370.
127. Wilson, W.G.; Heaslip, L.J.; Sommerville, I.D. Rare earth additions in continuously cast steel. *JOM* **1985**, *37*, 36–41. [CrossRef]

Disclaimer/Publisher's Note: The statements, opinions and data contained in all publications are solely those of the individual author(s) and contributor(s) and not of MDPI and/or the editor(s). MDPI and/or the editor(s) disclaim responsibility for any injury to people or property resulting from any ideas, methods, instructions or products referred to in the content.